CLM-P 467

SOME MAGNETIC FIELD DESIGN STUDIES FOR TOROIDALLY LINKED MIRROR SYSTEMS

C.J.H. Watson
Culham Laboratory, Abingdon, Oxon, OX14 3DB, U.K.
(Euratom/UKAEA Fusion Association)

1. Introduction

This paper considers the design of magnetic field configurations consisting of N minimum-B mirrors of the quadrupole type, linked toroidally to form a closed-line system. The reactor prospects of such 'toroidally linked mirror' (TLM) systems have been discussed in general terms in [1], where some preliminary designs were described. The present paper describes more recent developments in the design of such configurations. The most obvious design requirement is that the configuration should contain individual charged particles. In sections 2 - 4, we discuss analytic aspects of this question. In section 2, we neglect the effects of toroidal bending, and examine effects due to linking in an infinite straight chain of quadrupole mirrors. In section 3, we incorporate toroidal effects. In both sections, the analysis is restricted to the neighbourhood of the magnetic axis : however, as we show in section 4, such studies permit some general conclusions to be drawn about the constraints imposed by toroidal linking, and they indicate the region in parameter space where optimum configurations are likely to be found. In section 5 we apply these insights to the problem of designing an optimum layout of filamentary conductors of the yin-yang type, since the analytic studies show these to be superior to 'tennis ball seam' configurations. Although it is probable that yin-yang coils would be employed in a reactor, it can be argued that they are somewhat inconvenient for a preliminary experiment, and in section 6 we consider the design of coil layouts made up out of flat coils which, although sub-optimal, nevertheless generate usable TLM fields. Finally in section 7 we examine the factors which set a lower limit to the number of mirrors N in a TLM system, at the experimental and reactor level.

2. Analytic theory of particle orbits in straight-chain systems

In this section we consider an infinite chain of linked quadrupole minimum-B mirrors, and we restrict attention to the neighbourhood of the magnetic axis. Configurations of this type were first considered by Furth and Rosenbluth[2], who examined the stability of a low-β isotropic plasma in such a system. As they pointed out, the general expression for the magnetic scalar potential in the neighbourhood of a straight axis (in the z-direction) is :

$$\chi = B_o[f(z) - (x^2+y^2)f''/4 + (x^2-y^2)g(z)/2 + O(x^4, y^4)] \qquad (2.1)$$

where f and g are arbitrary functions of z only and $f' = \frac{df}{dz}$ etc.

The magnetic field on axis $\vec{B}(r=0) = B_o f'(z) = B_o b(z)$, and we choose B_o to be the minimum value of $\vec{B}$ on axis so that $b = 1$ at each minimum. The function b is assumed to be periodic, with period L, and to be symmetric about the plane $z = 0$ $(b = 1)$. The quadrupole term g is likewise assumed to be periodic, but with period $2L$, and is also symmetric about $z = 0$. It is normally more convenient to work with the antisymmetric function $c(z) = \int_o^z \frac{2g}{b}\,dz$ in place of g. In terms of b and c, the expression for $|B|$ is

$$|B|^2 = B_o^2 b^2 \left[1 + \frac{1}{4}\left(c'^2 + \left(\frac{b'}{b}\right)^2 - \frac{2b''}{b}\right)(x^2+y^2) + \frac{1}{2} c''(x^2 - y^2) \right]. \quad (2.2)$$

If one neglects terms of order x^2 and y^2 in the expressions for the field components, the equations defining the field lines can be integrated exactly, and give

$$x = \frac{Xe^{c/2}}{\sqrt{b}} \qquad y = \frac{Ye^{-c/2}}{\sqrt{b}} \quad (2.3)$$

where X and Y are constants, equal to the values of x and y at the plane $x = 0$.

The accuracy of eqns. (2.3) is nearly, but not quite, sufficient for X and Y to be Clebsch variables for the field (derived from (2.1), i.e. functions α, β such that

$$\vec{B} = \nabla\chi = \nabla\alpha \times \nabla\beta \quad (2.4)$$

In fact $\nabla X \times \nabla Y$ differ from $\vec{B}$ by terms of order x^2, y^2. With equal precision, one can take

$$\alpha = \tfrac{1}{2} B_o (X^2 + Y^2)$$
$$\beta = \tan^{-1} Y/X \quad (2.5)$$

as Clebsch variables, and we shall see that this represents a more convenient choice. It is straightforward to increase the accuracy of the expressions (2.5) so that they represent the field apart from terms of order x^4, y^4. One particular choice which satisfies this requirement is

$$\alpha = \frac{1}{2} B_o (X^2+Y^2)\left(1 - \frac{1}{8b}\left[(b'' + 2g')x^2 + (b'' - 2g')y^2\right]\right)$$
$$\beta = \tan^{-1} Y/X \quad (2.6)$$

Although in most of the following the distinction between (2.5) and (2.6) is not significant, to avoid confusion we shall denote by ψ the lower-order approximation to α, omitting for simplicity the constant factor $\frac{1}{2} B_o$ - i.e. we define

$$\psi = X^2 + Y^2 . \tag{2.7}$$

It follows from (2.4) and (2.6) that the α, β variables represent a non-orthogonal coordinate system labelling field lines : to specify a point in space, a third variable can be chosen variously as z (distance along the Cartesian axis), ℓ (distance along a field line) or χ (the scalar potential (2.1)). The advantage of choosing χ is that it alone is orthogonal to α and β.

Because of the symmetry of TLM configurations, they do not possess magnetic surfaces, except in the trivial sense in which any surface formed out of field lines passing through a prescribed closed curve in the midplane ($z = 0$) is a magnetic surface. Thus the merits of a given TLM field design depend upon the geometry of its guiding centre drift surfaces. These are the surfaces of constant J, the adiabatic invariant

$$J(\epsilon, \mu, \alpha, \beta) = \oint (\epsilon - \mu B(\alpha, \beta, \ell))^{\frac{1}{2}} d\ell \tag{2.8}$$

where ϵ is the particle energy, μ is its magnetic moment and the integral is taken between bounce points for trapped particles or around a closed line (or over one field period in the straight-chain limit) for passing particles. A necessary condition for adequate containment is that for most ϵ and μ, the J surfaces should be closed and nested about the axis. To evaluate J correct to order ψ, it is necessary to exercise some care because of the inequivalence (in this order) of $d\ell$ and dz. The simplest (and most illuminating) procedure is to expand

$$J = J_o + \psi \frac{\partial J}{\partial \psi} + O(\psi^2) \tag{2.9}$$

where

$$J_o = \oint (\epsilon - \mu B_o b)^{\frac{1}{2}} dz \tag{2.10}$$

and

$$\frac{\partial J}{\partial \psi} = \frac{\partial}{\partial \psi} \oint (\epsilon - \mu B(\psi, \beta, \ell))^{\frac{1}{2}} d\ell \Big|_{\psi = 0} = \frac{\partial}{\partial \psi} \oint (\epsilon - \mu B)^{\frac{1}{2}} \frac{d\chi}{B}$$

$$= \epsilon^{\frac{1}{2}} \oint W(b) \frac{1}{B_o} \frac{\partial B}{\partial \psi} dz \tag{2.11}$$

where $W(b) = b \frac{\partial}{\partial b}\left[\frac{\left(1 - \mu B_o \frac{b}{\epsilon}\right)^{\frac{1}{2}}}{b}\right]$ and the derivative $\frac{\partial B}{\partial \psi}$ is understood to be at constant β and χ, and is calculated as follows. Inserting (2.3) in (2.2) we have

$$B(X, Y, z) = B_o\left\{b + \frac{\psi}{8}\left[A \cosh c + 2c'' \sinh c\right] + \frac{X^2 - Y^2}{8}\left[A \sinh c + 2c'' \cosh c\right]\right\} \tag{2.12}$$

where $A = c'^2 + \left(\frac{b'}{b}\right)^2 - \frac{2b''}{b}$. We note that A is symmetric in z, whereas c and c'' are antisymmetric, and hence the first two terms in B are symmetric and the third antisymmetric. Since the range of integration of (2.11) is symmetric, we only require the symmetric part of $\frac{\partial B}{\partial \psi}$, which is given by

$$\frac{\partial B}{\partial \psi} \equiv \left.\frac{\partial B}{\partial \psi}\right|_{\beta,\chi,\text{symm.}} = \left[\left.\frac{\partial B}{\partial \psi}\right|_z + \left.\frac{\partial B}{\partial z}\right|_\psi \left.\frac{\partial z}{\partial \psi}\right|_\chi\right]_{\text{symm.}} = \frac{B_o}{8}\left[A + 2\left(\frac{b'}{b}\right)^2 \cosh c + 2\left(c'' - \frac{c'b'}{b}\right)\sinh c\right] \tag{2.13}$$

We note that this is a function of z only: thus $\frac{\partial J}{\partial \psi}$, and hence J itself (in the order to which we are working) is a function of ψ only - i.e. the drift surfaces are ψ surfaces, and intersect the midplane in a set of nested concentric circles.

This result suggests that TLM systems are 'omnigenic', in the sense of Hall and McNamara[3] - that the drift surfaces are independent of pitch angle. In fact, it is somewhat misleading in this respect; if one considers any system in which the high degree of symmetry implicit in (2.1) is broken in some manner - e.g. by introducing weak toroidicity or some small perturbation - one can show[4] that the drift surfaces have the form

$$\psi \frac{\partial J}{\partial \psi} + j(\psi, \beta) = \text{constant} \tag{2.14}$$

where j is of the order of the inverse aspect ratio, or the magnitude of the perturbation, and is therefore relatively small, except in a small range of pitch angles, described in [4] as the 'loss disc', in the neighbourhood of the point where $\frac{\partial J}{\partial \psi}$ goes to zero. From the Hamiltonian theory of bounce averaged guiding centre drift[5], one can identify this as the point

where the average azimuthal drift frequency goes to zero. In the neighbourhood of this point, the drift surfaces show large deviations from surfaces of constant ψ - thus any practical TLM system is only approximately omnigenic and great significance attaches to the loss disc, within which the drift surfaces become anomalous. However, because most particles drift on ψ surfaces, these do play a very important part in TLM theory, and for many purposes they can be regarded as analogous to the magnetic surfaces of toroidal configurations which lack the closed-line property.

It is convenient to introduce at this point some parameters associated with a given field configuration specified by $b(z)$ and $c(z)$. The overall mirror ratio on axis R is the maximum value of b: the mirror ratio along any field line other than the axis differs from R by at most a quantity of order ψ. If the configuration has a region of minimum-B, $\frac{\partial B}{\partial \psi} > 0$ at $z = 0$; on the other hand $\frac{\partial B}{\partial \psi}$ cannot be positive for all z, since this would violate Jukes' theorem[6]: thus $\frac{\partial B}{\partial \psi}$ must change sign at some point, which we shall loosly term 'the edge of the magnetic well', and we shall define R_W as the value of b at this point. Because $\frac{\partial B}{\partial \psi}$ is computed at constant χ and the χ surfaces are concave, the gradient of B perpendicular to the axis in fact changes sign at a slightly larger value of b, which we shall designate R_x. Specifically, since

$$B = b + \frac{1}{8} b\,[A \cosh c + 2c'' \sinh c]\, X^2 + \frac{1}{8} b\,[A \cosh c - 2c'' \sinh c]\, Y^2 \quad (2.15)$$

the perpendicular field gradient changes sign at $B = R_x$ for positive z in the Y direction, and for negative z in the X direction. A fourth mirror ratio, which is important in relation to the plasma distribution function, is the mirror ratio R_J at which particles with zero drift frequency reflect. From the above discussion, this occurs when $\frac{\partial J}{\partial \psi}$ given by (2.11) goes to zero. This expression is a weighted average of $\frac{\partial B}{\partial \psi}$ and changes sign at a value of $\frac{\epsilon}{\mu B_o} = R_J$ which is somewhat larger than R_W, and is often in practice quite close to R_x.

Finally, a parameter which plays an important role in the costing of a linked mirror system is the fanning ratio F, defined as the maximum displacement of a field line from the axis divided by its midplane displacement. From (2.3), we have

$$F = \frac{e^{C_{m/2}}}{\sqrt{R}} \qquad (2.16)$$

where $C_m = C(z = L/2)$. The shape of the surfaces of constant ψ at the mirror throat is given by

$$\left(x^2 e^{-C_m} + y^2 e^{C_m}\right) R = \psi = r_o^2 \qquad (2.17)$$

i.e. an ellipse with major radius of $F r_o$ and minor radius $\frac{r_o}{RF}$.

3. Analytic theory of orbits in toroidally linked systems

So far we have treated the magnetic axis as if it were essentially straight: we now consider the effect of introducing sufficient toroidal curvature for a system of N mirrors to close. For simplicity we shall restrict attention to the case of a flat magnetic axis (i.e. lying in a plane, which we shall denote by $z = 0$) and we shall introduce a locally orthogonal curvilinear coordinate system x, z, s, where s measures distance along the magnetic axis and x lies in the plane of the magnetic axis and is directed outwards. Let the local radius of curvature of the magnetic axis be $a(s)$. We now consider two ordering schemes: in the 'weak' ordering scheme we suppose that $\frac{x}{L} \sim \frac{L}{a} \sim \epsilon \ll 1$ everywhere, where L is the length between mirrors, whereas in the 'strong' ordering scheme we allow $\frac{L}{a} \sim 1$. The weak ordering is appropriate if the number of mirrors N is large and we bend the magnetic axis more or less uniformly, since then $\frac{L}{a} \sim \frac{2\pi}{N}$ and becomes small. In this ordering, the toroidal corrections to the field, which are of order $\frac{x}{a}$, become of order ϵ^2 and result exclusively from the metric coefficients occurring in the expression for the gradient operator - the corrections to the scalar potential χ are of order ϵ^3. The metric tensor is (cf. Solovyev and Shafranov[7] p. 27)

$$g_{ik} = \delta_{ik} \quad \text{unless} \quad i = k = 3$$
$$= \left(1 + \frac{x}{a}\right)^2 \qquad i = k = 3 \qquad (3.1)$$

$$g^{ik} = 0 \qquad i \neq k$$
$$= \frac{1}{g_{ik}} \qquad i = k \ . \qquad (3.2)$$

Thus the field line equations are of the form

$$\frac{dx}{B^x} = \frac{ds}{B^s} = \frac{ds\left(1+\frac{x}{a}\right)^2}{\frac{\partial\chi}{\partial s}} = \frac{d\ell}{B} \tag{3.3}$$

and hence

$$J = \oint (\epsilon - \mu B)^{\frac{1}{2}} d\ell = \oint (\epsilon - \mu B)^{\frac{1}{2}} \left(1+\frac{x}{a}\right)^2 B \Big/ \frac{\partial\chi}{\partial s}\, ds \ . \tag{3.4}$$

To evaluate (3.4) correct to order ϵ^2, it is sufficient to take the lowest order solution of (3.3)

$$x = \frac{Xe^{c/2}}{\sqrt{b}} \qquad z = \frac{Ze^{-c/2}}{\sqrt{b}} \tag{3.5}$$

and to write B in the approximate form

$$B = B_\infty \Big/ \left(1+\frac{x}{a}\right) + O(x^3) \tag{3.6}$$

(where B_∞ is in the form correct to x^2, z^2 in the limit $a \to \infty$). One then obtains

$$J = \oint (\epsilon - \mu B_\infty)^{\frac{1}{2}} d\ell + \oint \frac{\epsilon - \frac{1}{2}\mu B_\infty}{(\epsilon - \mu B_\infty)^{\frac{1}{2}}} \frac{x}{a}\, d\ell$$

$$= J_o + \psi \frac{\partial J}{\partial \psi} + \frac{X}{a} \oint \frac{\epsilon - \frac{1}{2}\mu B_o\, b}{(\epsilon - \mu B_o\, b)^{\frac{1}{2}}} \frac{e^{c/2}}{\sqrt{b}}\, ds \tag{3.7}$$

where $\psi = X^2 + Z^2$ and $\frac{\partial J}{\partial \psi}$ is the expression given by (2.11), with $\frac{\partial B}{\partial \psi}$ given by (2.13). The result, which is of the form (2.14), shows that in the weak ordering scheme, the drift surfaces remain concentric circles; the effect of toroidicity is to displace these centres outward by an amount

$$\Delta = \oint \frac{\epsilon - \frac{1}{2}\mu B_o\, b}{(\epsilon - \mu B_o\, b)^{\frac{1}{2}}} \frac{e^{c/2}}{\sqrt{b}}\, ds \Big/ \frac{\partial J}{\partial \psi} \tag{3.8}$$

which is small except within the loss disc, where $\frac{\partial J}{\partial \psi} \to 0$.

We now consider the strong ordering scheme. In this case we can still write

$$J = \oint (\epsilon - \mu B)^{\frac{1}{2}} \frac{\left(1+\frac{x}{a}\right)^2 B \, ds}{\frac{\partial \chi}{\partial s}} \qquad (3.9)$$

but now the terms proportional to x/a in this expression are generally of order ϵ and dominate over the terms proportional to ψ, which are of order ϵ^2. This leads to open drift surfaces, showing that toroidal curvature of this order is generally unacceptable. This conclusion can be avoided if $a(s)$ is chosen in such a way that this leading term is reduced in order. This can be achieved in two ways - either the sign of a is kept positive but its magnitude is made large except in regions where $x/\frac{\partial \chi}{\partial s}$ is exceptionally small, or the sign of a is made to alternate. The former option is adopted in the work described below, and amounts to bending the field sharply in the vertical fishtails of the quadrupole : the latter option has not been examined in detail, but looks less promising.

Within the strong ordering scheme, it is not immediately evident what is the appropriate form for the magnetic scalar potential χ. The difficulty lies in the fact that toroidal effects show themselves in terms of order x^3 and xz^2, and terms such as these also arise in the expansion of a field produced by hexapole windings in the neighbourhood of the axis. Since hexapole windings are qualitatively different from quadrupole windings (and less attractive from a reactor design viewpoint), we need some means of excluding hexapole terms from χ, while allowing strong toroidicity. This can be done as follows.

For clarity of exposition, it is convenient to consider first the case in which the radius of curvature of the magnetic axis is constant, even though (as we have just seen) this can only give rise to unacceptable toroidal effects. In this case we can immediately write down the exact general solution of Laplace's equation in terms of toroidal harmonics :

$$\chi = \bar{B} a \varphi + (\cosh \eta - \cos \tau)^{\frac{1}{2}} \sum_{m,n} A_{mn} Q^m_{n-\frac{1}{2}}(\cosh \eta) \cos n\tau \sin m\varphi \qquad (3.10)$$

where the A_{mn} and $\bar{B}$ are arbitrary constants. As noted in [1], if the limit circle of the coordinate system (a circle of radius a) is to be the magnetic

axis, the coefficients A_{m1} must be multiples of A_{mo}, chosen so that the coefficient of $\cos\tau$ in (3.10) vanishes in the limit $\eta \to \infty$. Otherwise the coefficients A_{mn} are free, and in particular the coefficients A_{mo} are the Fourier components of $\int_s b(s)ds$ (where $b(s)$ is the field strength on the magnetic axis), the coefficients A_{m2} are the Fourier components of the quadrupole term g, and coefficients A_{mn} for $n > 2$ give the magnitude of hexapole and higher order multipole components. This identification is unambiguous in the weak ordering scheme, where we can identify $\cosh\eta = \frac{a}{r}$ and $\tau = \theta$, where r, θ, s is a local cylindrical polar system: however even in the strong ordering scheme, the number of azimuthal nodes in the terms proportional to $\cos n\tau$ is equal to $2n$ showing that a conductor configuration with n pairs of opposing current elements (e.g. Joffe bars) is required to produce such terms. In this paper we have restricted ourselves (on the basis of engineering considerations) to quadrupole-type conductor configurations, and accordingly terms with $n > 2$ must be small or zero even when strong toroidal effects are present. To explore the implications of this restriction upon the expansion of χ near the magnetic axis, we note that apart from normalisation constants which can be absorbed into the A_{mn}, we have (Erdelyi [8] p.122)

$$Q^{m}_{n-\frac{1}{2}}(\cosh\eta) = \frac{\left(1 - \frac{1}{\cosh^2\eta}\right)^{m/2}}{\cosh^{n+\frac{1}{2}}\eta} F\left(\frac{m+n+\frac{1}{2}}{2}, \frac{m+n+3/2}{2}; n+1; \frac{1}{\cosh^2\eta}\right)$$

$$= \frac{1}{\cosh^{n+\frac{1}{2}}\eta}\left(1 + \frac{m^2 + (n+\frac{1}{2})(n+3/2)}{4(n+1)\cosh^2\eta} + O\left(\frac{1}{\cosh^4\eta}\right)\right) \quad (3.11)$$

and from the relationship between cylindrical polar coordinates $\rho\varphi z$ and toroidal coordinates (Hobson [9] p.434)

$$z = \frac{a\sin\tau}{\cosh\eta - \cos\tau} \qquad \rho = \frac{a\sinh\eta}{\cosh\eta - \cos\tau} \quad (3.12)$$

one can obtain

$$\frac{1}{\cosh^2\eta} = \frac{r^2}{a^2}\left(\frac{1+\frac{x}{a}+\frac{1}{4}\frac{r^2}{a^2}}{1+\frac{x}{a}+\frac{1}{2}\frac{r^2}{a^2}}\right)^2$$

$$\frac{\cos\tau}{\cosh\eta} = \frac{\frac{x}{a}+\frac{1}{2}\frac{r^2}{a^2}}{\left(1+\frac{x}{a}+\frac{1}{2}\frac{r^2}{a^2}\right)} \qquad (3.13)$$

where $x = \rho - a$ and $r^2 = x^2+z^2$. Inserting (3.11) and (3.12) in (3.13), and setting $A_{m1} = \frac{1}{2} A_{mo}$ (so that the terms in χ which are linear in x/a vanish), we obtain on expansion

$$\chi = \bar{b}s + \frac{1}{\left(1+\frac{x}{a}+\frac{1}{2}\frac{r^2}{a^2}\right)^{\frac{1}{2}}} \sum_m \Big[A_{mo}\left(1+\frac{m^2+\frac{3}{4}}{4}\frac{r^2}{a^2}\left(1-\frac{x}{a}\right)+\frac{\frac{1}{2}\frac{x}{a}+\frac{1}{4}\frac{r^2}{a^2}}{1+\frac{x}{a}+\frac{1}{2}\frac{r^2}{a^2}}\left(1+\frac{m^2+\frac{15}{4}}{8}\frac{r^2}{a^2}\right)+O\frac{r^4}{a^4}\right)$$

$$+ A_{m2}\frac{2\left(\frac{x}{a}+\frac{1}{2}\frac{r^2}{a^2}\right)^2 - \frac{r^2}{a^2}\left(1+\frac{x}{a}\right)}{\left(1+\frac{x}{a}+\frac{1}{2}\frac{r^2}{a^2}\right)^2}\left(1+\left(\frac{m^2}{12}+\frac{35}{48}\right)\frac{r^2}{a^2}\left(1-\frac{x}{a}\right)\right)\Big] \sin m\varphi$$

$$= \sum_m \Big\{ A_{mo}\left[1 - \frac{3}{16}\frac{(x^2-z^2)}{a^2} + \frac{m^2}{4}\frac{r^2}{a^2} + \frac{5}{8}\frac{x^3}{a^3} - \frac{27}{64}\frac{xr^2}{a^3} - \frac{5}{16}m^2\frac{xr^2}{a^3}\right]$$

$$+ A_{m2}\left[\frac{x^2-z^2}{a^2} - \frac{3}{2}\frac{x^3}{a^3} + \frac{7}{2}\frac{xz^2}{a^3}\right]\Big\} \sin m\varphi$$

$$= \left(\int_s b\,ds + Ax^2 + Bz^2 + Dx^3 + Fxz^2\right) \qquad (3.14)$$

where $A = -\frac{3}{16a^2}\int_s \tilde{b}\,ds - \frac{b'}{4} + \frac{g}{2}$ $\qquad B = \frac{3}{16a^2}\int_s \tilde{b}\,ds - \frac{b'}{4} - \frac{g}{2}$

$$D = \frac{13}{64a^3}\int_s \tilde{b}\,ds - \frac{3}{4}\frac{g}{a} + \frac{5}{16}\frac{b'}{a} \qquad F = -\frac{27}{64a^3}\int_s \tilde{b}\,ds + \frac{7}{4}\frac{g}{a} + \frac{5}{16}\frac{b'}{a}$$

$$\tilde{b} = b - \oint b\,ds/\oint ds = b - \bar{b}\,.$$

We may note in passing that these coefficients satisfy identically the relations

$$2A + 2B + b' = 0$$

$$\frac{2A}{a} + 6D + 2F - \frac{2b'}{a} - \frac{ba'}{a^2} = 0 \qquad (3.15)$$

obtained by McNamara[10] by expanding Laplace's equation in the neighbourhood of a curved magnetic axis (and the equivalent set derived by Solovyev and Shafranov[7]). However our expressions contain only two free functions b and g, whereas in the analysis of McNamara D and F were also free functions.

The extension of the above analysis to allow for a magnetic axis of variable curvature (but still lying in a plane) is trivial. As (3.15) shows, the potential given by (3.14) now fails to satisfy Laplace's equation to the order in which we are working by a term $-\frac{ba'x}{a^2}$. To cancel this term we need to add a suitable term to either A, B, D or F. There is some freedom at this point, and for simplicity we choose to add $\frac{1}{6}\frac{ba'}{a^2}$ to D.

Using equation (3.14) one can obtain solutions of the field line equations in the appropriate approximation and insert them into (3.9) to determine the drift surfaces. We do not carry out this analysis here, since we only require qualitative features of the result, which are already evident. The drift axis is displaced outwards by an amount which is still given in adequate approximation by (3.8). However, the shapes of the drift surfaces now show a significant ellipticity and triangularity, since the terms of order $\frac{x^2}{a}$ and $\frac{xz^2}{a}$ in χ are now of the same order in ϵ as the terms of order x^2 and z^2 which generate the term $\psi\frac{\partial J}{\partial \psi}$. Conversely, in order to minimise both the toroidal displacement Δ and the deviation from omnigenicity, the field designer should arrange for the magnetic axis to approach a polygon as closely as possible - i.e. to make it piecewise straight $(a \to \infty)$ with localised regions of sharp bending, located where $e^{c/2}/\sqrt{b}$ is as small as possible. In the following section we assume that this has been done.

4. Optimisation of field profiles

We have seen that in both straight-chain and toroidally linked quadrupole mirror systems with a suitably specified magnetic axis, the magnetic field configuration is determined by two periodic scalar functions b and g. We now consider the optimisation of the profiles b(s) and g(s). A tempting starting point is the line of reasoning given in an earlier paper on ordinary mirror reactor design[11] in which it was supposed

that the magnetic field windings are distributed smoothly over a suitable magnetic surface, and it was concluded that from an economic standpoint the optimum configuration was one in which $\left.\frac{\partial B}{\partial \psi}\right|_z$ was arranged to be very slightly greater than zero for all z up to R, a condition which determined both the profile of $b(z)$ and the fanning. We have some reservations about the validity of that analysis, since in view of the distinction made in section 2 between $\left.\frac{\partial B}{\partial \psi}\right|_z$ and $\left.\frac{\partial B}{\partial \psi}\right|_\chi$, the condition $\left.\frac{\partial B}{\partial \psi}\right|_z > 0$ is, strictly speaking, neither necessary nor sufficient for stability of a mirror-confined plasma (though it not likely to be seriously in error). However it led us to examine the analogous problem generated by the analysis of the present paper, the determination of the profiles of b and g which satisfy the condition $B = B(\psi, z)$, $\left.\frac{\partial B}{\partial \psi}\right|_\chi = 0$ for all z up to some R_W. These two conditions can be expressed in the form:

$$\left[c'^2 + \left(\frac{b'}{b}\right)^2 - \frac{2b''}{b} \right] \sinh c + 2c'' \cosh c = 0 \quad \text{(antisymmetric part of } B = 0\text{)}$$

$$\left[c'^2 + \left(\frac{b'}{b}\right)^2 - \frac{2b''}{b} \right] \cosh c + 2c'' \sinh c + \frac{2b'}{b}\left(\frac{b'}{b}\cosh c - c' \sinh c\right) = 0 \quad \left(\left|\frac{\partial B}{\partial \psi}\right|_\chi = 0\right). \tag{4.1}$$

We can simplify these equations by taking c as the independent variable; writing $b = b(c)$, $\dot{b} = \frac{db}{dc}$, $b'' = \ddot{b}\, c'^2 + \dot{b} c''$ etc., we find that c' and c'' can be eliminated altogether, and we obtain a non-linear differential equation of the Abel type for b:

$$1 + \left(\frac{\dot{b}}{b}\right)^2 - 2\frac{\ddot{b}}{b} = 2\frac{\dot{b}}{b}\left(\frac{\dot{b}}{b}\sinh c - \cosh c\right)\left(\frac{\dot{b}}{b}\cosh c - \sinh c\right) \tag{4.2}$$

Transforming to $x = \cosh c$ as independent variable, and $p = \frac{db}{dx}/b$ as dependent variable we obtain

$$\frac{dp}{dx} = -x(x^2-1)p^3 + \left(\frac{4x^2-3}{2}\right)p^2 - \frac{x^3}{x^2-1}p + \frac{1}{2(x^2-1)} \quad . \tag{4.3}$$

We have solved (4.3) numerically with boundary conditions $b(o) = 1$, $\dot{b}(o) = 0$, and find that as c becomes large, b saturates in such a way that xp becomes small. In this limit we can expand (4.3):

$$\frac{dp}{dx} \simeq \frac{1}{2x^2} - xp \tag{4.4}$$

which has the solution

$$p = p_1 e^{\frac{x_1^2 - x^2}{2}} + \frac{1}{2} e^{-\frac{x^2}{2}} \int_{x_1}^{x} \frac{e^{\frac{x^2}{2}}}{x^2} dx$$

$$\simeq \frac{1}{2x^3} + O\left(\frac{1}{x^4}, e^{-\frac{x^2}{2}}\right) \tag{4.5}$$

Thus asymptotically

$$\frac{d \ell n b}{dx} \to \frac{1}{2x^3}$$

and hence

$$b \to b_{max} e^{-\frac{1}{4x^2}} \tag{4.6}$$

where b_{max} is a constant not given by this asymptotic analysis, but which is computationally equal to 1.766. Equation (4.6) accurately represents the form of b(c) for large c obtained from computations with (4.2). It shows that for $R_W > 1.766$ it is impossible to achieve a magnetic well by marginally satisfying the condition $\left.\frac{\partial B}{\partial \psi}\right|_\chi = 0$ everywhere. (By contrast, the weaker condition $\left.\frac{\partial B}{\partial \psi}\right|_z = 0$ led to a trivial solution to the equations corresponding to (4.1) for all values of R_W.)

This result does not exclude the possibility of configurations with $R_W > 1.766$: indeed we shall shortly obtain examples of such configurations (in which the profiles of $\frac{\partial B}{\partial \psi}$ attained quite large positive values, and hence are not even approximately described by the condition $\frac{\partial B}{\partial \psi} = 0$). However it excludes the use of the strategy of the earlier paper to determine the profiles of b and g . Instead, we have made a fairly extensive exploratory study, using Fourier series to represent b and g , the series being truncated before the point at which the number of independent parameters becomes unmanageably large :

$$b = \frac{R+1}{2} - \frac{R-1}{2} \cos 2t \tag{4.7}$$

$$g = \frac{\pi}{4L} (C_1 \cos t - 9 C_3 \cos 3t) \tag{4.8}$$

where $t = \pi z/L$. (The normalisation of the coefficients C_1 and C_3 is chosen to facilitate comparison with the results of [1]). This choice of b and g gives

$$c = \frac{18\,C_3 \sin t}{R-1} + \frac{1}{2}\,(C_1 - 9\,C_3 - 36\,C_3/(R-1))\tan^{-1}(\sqrt{R-1}\sin t)/\sqrt{R-1}\,. \quad (4.9)$$

Of the three parameters specifying this configuration, R has an obvious physical meaning, but C_1 and C_3 do not. To give some insight into their significance, it may be remarked that provided that C_1 and C_3 are chosen so that the configuration has an absolute minimum in B at $z = 0$ (a condition which may be written in the form

$$C_1 - 9_3C_3 \geq 4(R-1)^{\frac{1}{2}} \quad (4.10))$$

the fanning ratio F is almost independent of C_3, so that for given R, the parameter C_1 determines F. The parameter C_3 can then be used to shape the profile of g away from the plane $z = 0$, and hence to vary the mirror ratio R_W at which $\frac{\partial B}{\partial \psi} = 0$. Thus equivalently the configuration may be considered to be determined by the values of R, F and R_W, although for a given R, the range of attainable values of F and R_W are somewhat restricted since there is a minimum value of F and a maximum value of R_W. (We could equally well use R_J in place of R_W as the third parameter: however this would slightly complicate the discussion below without altering the conclusions since, as we shall see, R_J and R_W are closely related).

The determination of F and R_W for given C_1 and C_3 is a straightforward computational matter and we present the results in figs. 1 and 2 for $R = 2$ and $R = 3$ respectively. In each case the upper solid curve indicates the limit defined by (4.10): above this line $\frac{\partial B}{\partial \psi} < 0$ at the midplane, so R_W does not exist. It is seen that the value of R_W on this limiting curve increases monotonically with C_1 (i.e. with the fanning ratio F) and saturates at $R_W/R \sim 90\%$. However there is a minimum value of the fanning given in good approximation by (cf. (4.9) and (4.10))

$$F_{min} = \frac{e^{\tan^{-1}\sqrt{R-1}}}{\sqrt{R}} \quad (4.11)$$

below which no magnetic well is obtainable at all. To obtain a reasonable magnetic well, a slightly greater fanning is required, and we have given some attention to the question whether an optimum degree of fanning exists.

It appears that this question can most readily be answered by considering the manner in which any given profile of $\frac{\partial B}{\partial \psi}$ might be produced. In fig. 3 we illustrate the required profiles for various values of C_3 at constant R and C_1 (and hence constant fanning $F = 3$). It is seen that if the task were simply to maximise R_W/R, regardless of magnet cost, one would set $C_3 = 0.482$, giving $\frac{\partial B}{\partial \psi} = 0$ at the midplane and a large positive value of $\frac{\partial B}{\partial \psi}$ near $b = R_W$. However the need for a large quadrupole component near $b = R_W$ would certainly lead to large forces on the windings, and hence to a relatively expensive magnet structure. By contrast, the value $C_3 = 0.3$ gives such a low value of R_W/R that the same value of R_W could surely be obtained more economically in a system with a smaller value of R. The intermediate case $C_3 = 0.4$ gives a rather low flat profile of $\frac{\partial B}{\partial \psi}$, but a value of R_W somewhat less than the maximum obtainable at that fanning. Thus the economically optimum profile lies somewhere between the flat profile given by $C_3 = 0.4$ and the peaked profile given by $C_3 = 0.482$, the optimum being determined by the manner in which the magnet cost scales with F and R for given R_W. For orientation, the lower solid curve in figs. 1 and 2 gives the value of R_W produced by 'flat' $\frac{\partial B}{\partial \psi}$ profiles (in the sense that $\frac{\partial^2}{\partial z^2}\frac{\partial B}{\partial \psi} \simeq 0$ and $\frac{\partial B}{\partial \psi}$ is monotonically decreasing away from the mid plane).

A rather crude estimate of the manner in which the magnet cost scales with F and R for given R_W can be obtained as follows. It is qualitatively clear that $\frac{\partial B}{\partial \psi}$ profiles of the required shape can be obtained using tennis ball seam or yinyang coils. The former tend to produce rather flat $\frac{\partial B}{\partial \psi}$ profiles, and the latter give relatively peaked profiles. In both cases, coils of given overall size, producing the same central magnetic field B_o, contain a roughly constant amount of superconductor, so that the cost variations are due primarily to variations in the structure required to withstand the forces on the windings. The most serious forces are the repulsive forces between those parts of the windings which generate the field in the mirror throats. The restraining structure for these forces can be approximated by a pair of straight beams subjected to a uniform pressure loading of $(RB_o)^2/8\pi$ along the whole of their unsupported length of $F r_o$, where r_o is the radius of the outermost flux surface at the midplane (which we take as constant). If these beams were rectangular section beams of length ℓ and depth d, the maximum stress † would scale as $(\ell/d)^2$ and hence the deflection ϵ as ℓ^4/d^3. It is natural to restrict ϵ to a constant fraction of ℓ, so that $\frac{\epsilon}{\ell} \sim (\frac{\ell}{d})^3$ is constant and

† We are indebted to Mr A.P. Pratt and Mr J.D. Mitchell for the argument at this point.

hence d scales as ℓ. Hence the volume (and cost) of the structural material scales as $\ell d = \ell^2$ for fixed R and hence scales as $(FR)^2$ where F and R are varied at fixed B_o and r_o. It is clear from dimensional considerations that the same scaling law would apply to restraining structures other than rectangular bars provided that their geometry is held constant.

Using $(FR)^2$ as the optimisation function, we have calculated its variation with R for given R_W for a range of R_W values, taking for definiteness the peaked $\frac{\partial B}{\partial \psi}$ profile. The results are shown in fig. 4. It is seen that, for given R_W, the function $(FR)^2$ has a rather flat minimum as a function of R. However this minimum value of $(FR)^2$ increases rather rapidly with R_W (almost as R_W^4) so it is likely that in an optimised reactor design (in which the scaling of the plasma containment with R_W is taken into account) the R_W value is likely to be quite low. (It has to be borne in mind that the above discussion relates to the vacuum magnetic field, which is of primary importance in stability discussions, whereas the containment time scales with the self-consistent mirror ratio, taking the plasma into account). The optimum fanning is rather constant in the range of R_W values considered here, and lies between 2.6 and 3.2.

Throughout the above discussion we have used R_W rather than R_J as a measure of the magnetic well depth. For most purposes they are essentially equivalent, since, as figs. 1 and 2 show, they depend in a similar manner on the constants C_1 and C_3, and R_J exceeds R_W by a nearly constant amount.

These analytic studies are restricted to the neighbourhood of the magnetic axis, and consequently do not give a complete picture of the properties of a magnetic configuration produced by a finite conductor layout. Nevertheless, they indicate constraints which any real field must satisfy - e.g. the relationship between R_W and F, the approximate scaling of the cost of an optimised magnet with R_W, and the desirability of a peaked $\frac{\partial B}{\partial \psi}$ profile. Consequently in the work described in the following section, we set ourselves the objective of finding simple conductor configurations of the yin yang type which give fanning ratios in the range 3 to 4, for overall mirror ratios in the range 2 to 3, aiming at a well mirror ratio $R_W \sim 1.5$ for $R = 2$, or $R_W \sim 1.9$ for $R = 3$.

5. Toroidally linked yin yang configurations

A yin yang coil represents a reasonable approximation to the distributed current sheet which would generate an ideal magnetic well with a peaked $\frac{\partial B}{\partial \psi}$ profile. The quadrupole component of the field is somewhat localised in the mirror throats, because that is where the windings are located, so the

g profile automatically possesses the favourable shape mentioned in the preceding section. For these reasons, we concentrate in the first instance on the design of a system of linked yin yang mirrors.

The basic problem in the optimisation of such systems is the very large parameter space involved. To reduce this to a minumum without a significant loss of generality, we first defined a geometrically idealised yin yang winding, with all curvature eliminated. This rectangular yin yang configuration is illustrated in fig. 5 which shows both a plane and conical projection. The yin and yang windings are identical : each is defined by a height H , width W , length L and angle A as indicated and they are separated by a distance S . Naturally, in a final engineering design it would be necessary to restore the curvature ; however we do not believe that the resulting fields would be significantly different except in the immediate neighbourhood of the windings. For fixed S , the range of values of H W L A which produce a minimum-B field of given mirror ratio is surprisingly limited. These values are not reported here, since they are irrelevant to TLM design because of the strong interaction between adjacent mirrors.

In the first instance, we examined the design of a configuration consisting of 8 mirrors. This choice was influenced by the fact that in an earlier study[1], it had been found possible to achieve a nearly square magnetic axis in an 8-mirror system, with all the curvature localised in the vertical mirror throats, and with reasonably small residual toroidal effects. The question of the feasibility of reducing this number is examined in section 7.

To form an 8 mirror system, the yin yangs are laid out in four pairs, each pair having their magnetic axis coincident and the two adjacent fish-tails horizontal. The separation D of two adjacent windings is a further parameter. The four pairs are then arranged so that their axes form a square and a "bending coil" (an elliptical, or in the present idealised scheme, a rectangular coil of width w and height h) is added at each corner to guide

the magnetic flux round. A typical coil layout is shown in fig. 6. The need for bending coils is not proven at this stage in TLM theory: however in their absence there are four additional non-minimum-B mirrors at the four corners, and these may have unfavourable effects on the stability of the configuration.

We first examined the interaction of the fields of one pair of yin yangs. As would be expected, if H W L and A are held constant and D is decreased, the interaction becomes significant when D becomes of order W . The effect is unfavourable: the interaction reduces the depth and axial extent of the magnetic well produced by each yin yang. It also increases the mirror ratio. On the other hand, if D is much larger than W , there is a substantial dip in B between the mirrors, and for the stability reasons mentioned above we have judged this undesirable. In view of the uncertainty about its effect on stability, we have adopted a rather arbitrary compromise on this point, taking $D = 0.32\ S$. This gives a dip of less than 15% in the value of B on axis between the mirrors, and has a relatively weak effect on the magnetic wells.

In the layout of the four pairs of yin yangs we have also made a somewhat arbitrary compromise, for similar reasons. We have found that if the mean separation of the adjacent vertical yin yang coils is also about $0.32\ S$, this is in practice just sufficient to avoid overlap of the coils at their points of closest approach, at least in the optimised designs described below, and it again gives an acceptably small interaction between adjacent magnetic wells. These conventions are incorporated in the layout shown in fig. 6. In this figure, the scale can be interpreted as metres for a possible TLM reactor configuration. In this case, and indeed in all our yin yang computations, we have taken $S = 7.5$ m and fixed the centre of the first yin yang at the point (4.0, -11.0, 0.0) metres, which gives a magnetic axis in the form of a square of side 21 m. The width of the bending coils w was then chosen as 2 m to give a field having the range of the dip found

computationally to occur without it, and the first such coil was positioned so that the inner vertical was slightly inside the point (0, -15, 0) at which the corner of a perfectly square magnetic axis would be situated. Thus this bending coil intersects the mid plane at the points (0, -14.5) and (0, -16.5). Their height was arbitrarily chosen to be $h = 10$ m so that end effects were unimportant: this could be reduced in a fully realistic design. The current was fixed at $\frac{1}{3}$ of the yin yang current.

With this layout fixed, we then varied HWL and A systematically in order to determine optimum values, adjusting the yin yang current I to the level required to give a field of 1 Tesla at the minimum. In each run we computed B on the magnetic axis and on lines displaced by a perpendicular distance of 0.5 m in the vertical and horizontal directions, and we followed two field lines from the points (4.25, -10.25) and (4.75, -10.75), chosen because in typical cases they lay in or close to the plane in which the minimum is found to occur. From the printout we could obtain the overall mirror ratio R (taken for definiteness as that at the horizontal fishtail, since the other can be adjusted with the help of the bending coil), the radial well depth Δ (defined as the minimum value of the perpendicular difference ΔB between the field on the displaced lines and the field on the axis in the neighbourhood of the minimum-B), the fanning ratio F, and an approximate value ($\pm$ 20%) of the mirror ratio R_x at which $\nabla_\perp B$ changes sign (where $\nabla_\perp$ is taken in the most unfavourable direction perpendicular to the magnetic axis). Some preliminary runs showed that for fixed H, W had a large effect on R and only a weak effect on F and Δ, whereas L and A had a large effect on F and Δ and only a weak effect on R. Thus our procedure became as follows: fix H arbitrarily, vary A systematically, choose L so that $\Delta \simeq 0.02$ and then find values of W such that $R \simeq 2$ and $R \simeq 3$. The results are shown in table 1.

The most significant results are as follows.

(i) For $H \leq 6$ it is impossible to produce configurations with reasonable fanning ratios. This is because it is necessary to have a large radial well near the mirror throat in order to have any well ($\Delta = 0.02$) near the minimum, and any unnecessarily large radial well depth enhances the fanning.

(ii) Conversely, for $H = 8$ one already achieves almost the minimum fanning consistent with given R_x (cf section (4)).

(iii) For fixed H, F increases with R_x in roughly the manner expected from analytic studies.

(iv) In order to achieve the design targets set in the introduction, the relevant region of parameter space is quite small: $7 < H \lesssim 8$, $5.0 \leq L \leq 5.5$, $100^0 \leq A \leq 110^0$.

As an illustration of the magnetic field profile obtained from these configurations, we give in fig. 7 contour plots of B in the plane $z = 0$ and superposed plots of field lines which lie in that plane, for two of the configurations (labelled 8Y2 and 8Y3 in the table). These plots show some features of interest. (a) Although the mirror ratio R_W (or R_x) is rather independent of the field line, the overall mirror ratio varies rather more, and the depth of the dip in B between mirrors varies enormously. It is not possible to avoid this dip: it is necessary in order that this toroidal configuration should satisfy Jukes' theorem[6]. (b) The fanning ratio increases with distance away from the axis, and eventually goes to infinity (i.e. the configuration has a separatrix.) We have not attempted to locate the separatrix in detail in these studies, since in any realistic system it would be necessary to add small trimming coils to control its location and divert escaping plasma. However in order of magnitude, the separatrix radius at the minimum-B plane (hereafter called the 'midplane') is 70 cm, so a reactor might possibly need to have dimensions somewhat scaled up from those indicated here, though it may be possible to increase the separatrix radius, without changing the coil dimensions, with the help of trimming coils at the edges of the fishtails to

compress the flux there. (c) It is seen that there is room to insert an adequate thickness of neutron blanket inside coils even without further scaling up, though in the fishtails (where the neutron flux would in any case be relatively small) its thickness would need to be the minimum required for magnet protection. (d) The overall coil dimensions do not give an accurate estimate of the lengths of the unsupported spans of conductor subject to forces. There is room for supporting structure in places. However the magnetic flux surfaces do define a volume within which no structure is permissible. In this respect, TLM systems (in which good containment of passing particles is essential) are perhaps different from individual mirror systems, where it has been argued[12] that one might allow magnetically protected structural pillars to perforate the fishtails and accept the residual level of plasma bombardment. Because the overall fanning ratio does not determine the span of structural material, the estimate of the scaling of the cost of the magnet given in section (4) is not very precise, though it is probably qualitatively correct. Some indication of the support structure which would be required can be obtained from the FERF design for a single yin yang coil[13]: the linear dimensions shown in fig. 6 are all approximately 50% larger than FERF. (e) It is clear that there is no linking of coils in this TLM design: each coil could be withdrawn independently for maintenance or replacement.

6. Toroidally linked tennis-ball seam configurations

For the reasons already given it seems probable that a reactor system would use yin yang coils. However these are undoubtedly difficult to fabricate to the required tolerances, and present serious geometric problems in the design of support structures. There is thus an incentive to look for something simpler which is capable of producing a comparable magnetic well. Such a configuration might well have a role in earlier experiments, or in a prototype reactor. In the search for such a configuration, we observed that if one attempts to 'rectangularise' a tennis-ball seam winding in the same

manner as was used above to rectangularise a yin yang, the resulting structure can be broken up into three flat coils if one is prepared to accept a moderate amount of current cancellation. (See fig. 8). We have therefore examined the design of TLM systems based upon this configuration.

As before, an individual tennis-ball seam coil is defined by the minimum number of parameters by making suitable symmetry assumptions - the minimal set are the height H, the length L and the gap G through which the fishtails emerge, and are indicated in fig. 8. To facilitate comparisons with the yin yang configuration, we chose that the magnetic axis should be identical (i.e. the square formed by joining the points (0 ± 15) and $(\pm 15, 0)$) and that the geometric centres of the tennis-ball seam coils should again be situated at the same points $(4, -11)$ etc. We then carried out some preliminary computer studies to determine a suitable value of L, having regard to the dip in B between adjacent mirrors, and fixed on $L = 6$ m as giving a reasonable compromise. On exploration, it then turned out that in reasonable approximation, the gap G determined the mirror ratio R and the height H determined both the depth of the magnetic well Δ and the fanning ratio F. We therefore chose values of G which gave $R = 2$, 2.5 and 3, and varied H systematically. The results are shown in table 2. (In this case, F is defined by field lines starting at the points $(3.95, -10.95)$ and $(4.45, -11.45)$: these are not symmetrically distributed about the geometric axis of the coils, reflecting the fact that the magnetic axis in this configuration is somewhat displaced with respect to the geometric axis.) The B contours and field lines for representative configurations (labelled 8T2 and 8T3 in table 2) are shown in fig. 9.

Some features of these results may be noted:

(a) The fanning ratio varies with Δ (and H) in the manner that one would expect. The principal effect of varying H is to move the 'Joffe bar'

component of the winding with respect to the magnetic axis: in order to keep Δ to a minimum, it is necessary to make H quite large. At this minimum, the fanning ratio F is very comparable with the fanning in the equivalent yin yang configuration.

(b) By contrast, the value of R_x is markedly inferior. This reflects the fact that the quadrupole profile $g(s)$ produced by a tennis-ball seam configuration is rather flat, instead of being peaked near the mirror throat, and as shown above this leads to an inferior magnetic well. However it is not overwhelmingly inferior, and the greater simplicity of this design might lead to its being preferred.

(c) As in the yin yang configuration, the overall dimensions of the coils give a misleading impression of the required span of unsupported conductor. The overall dimensions are rather larger than the corresponding yin yang configuration: however if this were significant, the dimensions could probably be reduced by increasing the number of coils from three to four and varying the ratios of the currents in them.

7. Four-mirror TLM configurations

Although it has been argued[1] that eight is an acceptable number of mirrors in a TLM reactor, there may be economic advantages at the reactor level, and there are certainly practical advantages at the level of preliminary experiments, in reducing the number of mirrors below eight, if this is possible without a significant loss of performance. The minimum number of quadrupole mirrors which can be linked in a manner which has sufficient symmetry to give a closed field-line configuration is four, and we have examined the design problems raised by reducing the number of mirrors to this limit.

We first considered a system of 4 yin yang mirrors. It was necessary at the outset to determine whether any significant degree of bending at the horizontal fishtails was permissible. We therefore started with the 8Y2

yin yang configuration described in section 2 and arranged two pairs with their axes tilted 45° away from coincidence, in the manner indicated in fig.10. Two bending coils, intersecting the symmetry plane at the points (± 9.0) and (± 12.0) were also added. The resulting B contours and field line are shown in fig.11. It is seen that even this modest degree of tilting of the axes, which is by no means sufficient to make the bending coils superfluous, is sufficient to produce a substantial toroidal distortion of the field lines. The shortest field line, (which defines the centre of the drift surfaces for passing particles) instead of being the central one, is now almost at the edge of the configuration. We concluded that no significant amount of tilting was acceptable.

We then examined the consequences of laying two coaxial pairs side by side, placing them with their centres at (± 4.75, ± 4) - i.e. as close to each other as possible without coil overlap, and adding a single bending coil to guide the flux around each of the two vertical fishtails. The parameters for each yin yang were the same as in the 8Y3 system - HWLA = 8 , 2.2 , 5 , 110 . The location and dimensions of the bending coils were chosen empirically to give a good compromise between minimum toroidal effects in the minimum-B regions and minimum fall-off in the field strength within the linking sections. The chosen parameters were h = 10 m , w = 5 m , with intersections at (7,0) and (12,0). This configuration is shown in fig. 12, and it gives the B contours and field lines plot shown in fig. 13.

Comparing this with fig. 7 for the 8Y3 configuration, it is seen that the B contours are qualitatively similar. However closer inspection of fig. 13 reveals toroidal effects which are not present in fig. 7 : the B contours are displaced away from the axis and break open rather sooner, and the central field line is appreciably curved even within the closed B contours. This is due partly to the interaction between adjacent yin yang fields, and partly to

the effect of the bending coils. It is not obvious from fig. 13 whether these effects are acceptable : however a study of the J contours defining the drift orbits in this system (which will be reported in more detail elsewhere[14]) has shown that they are unacceptable. Even particles reflecting at the surface with $R = 1.3$ are grossly shifted away from the magnetic axis, and those reflecting at $R = 1.4$ have uncontained drift orbits. This result can be understood with the help of eqn. (3.7) as due to the sensitivity of the drifts of particles close to the loss disc to small toroidal effects, since $\frac{\partial J}{\partial \psi}$ is small for these particles.

To eliminate the effect of interaction of adjacent yin yangs, the separation between the two axes was increased from 8 to 14 metres (this increase was found to decouple the two pairs of yin yangs almost completely : it is possible that in an optimised design a somewhat smaller increase would be found sufficient). To guide the flux around the linking section without introducing either unacceptable toroidal effects within the mirrors, or a large drop in field strength within the links, it then proved necessary to introduce four bending coils in each link : after some experimentation suitable parameters were found to be $h = 10$ m, $w = 3$ m, with their centres at $(\pm 11.5, \pm 1.5)$ and $(\pm 11.5, \pm 4.5)$. This coil layout is shown in fig. 14. The choice of the optimum parameters for one yin yang coil proved to be a matter of some delicacy. The parameters chosen for the configuration 8Y3 - HWLA = 8, 2.2, 5, 110 - turned out to give a rather large fanning ratio for the outermost flux surfaces ($F \gtrsim 5.5$) and correspondingly a rather poor drift separatrix radius in the midplane for passing particles (~ 55 cm), although it was very satisfactory from the point of view of trapped particles. As table 1 shows, one can improve the fanning ratio at the expense of R_W by decreasing the angle A : however because of the importance of minor toroidal effects, the 4-mirror configuration is more sensitive to A than the 8-mirror configuration, and we found that although reducing A from 110 to 105° reduced

the fanning from 5.5 to 3.8, it already had an excessive effect on R_W; it gave butterfly orbits for particles reflecting at $R = 1.4$ and unfavourable drifts for particles reflecting at $R = 1.6$. Interpolating between these limits, we found a reasonable compromise configuration with the parameters HWLA = 8, 2.3, 5, 107, $I_{\text{yin yang}} = 7\,\text{MA}$, $I_{\text{bending}} = 7.5\,\text{MA}$: the B contours and field lines are shown in fig. 15. From the J contours, it can be inferred that this configuration, which we designate TLM 4Y3, has a value of $R_W \simeq 1.7$, and a fanning ratio $F \simeq 3.7$ for field lines starting at a radius of 35 cm.

We finally considered a system of four tennis-ball seam coils. As in the yin yang case, we arranged these in pairs with a straight axis, and added bending coils as necessary to minimise the dip in B in the linking regions. As in the yin yang case, our initial layout had the two pairs as close as possible without coil overlap, and we were forced, because of the observed toroidal effects, to increase the separation. By contrast with the yin yang case, however, reasonable separations proved insufficient to reduce the interaction between the adjacent coils to an acceptable level. For example, when the separation of the axes and the layout of the bending coils are as in TLM 4Y3, and the individual tennis-ball parameters are as in 8T3, even particles reflecting at $R = 1.4$ are on uncontained drift orbits, and an increase in the separation of the axes from 14 to 16 m produces no detectable improvement in the B contours. We confirmed, by removing the bending coils altogether, that this behaviour is due to the toroidal effects resulting from the field of the adjacent tennis-ball coils. The difference between the tennis-ball and yin yang coils in this respect is due to the much greater separation of the currents generating the quadrupole component of the field in the tennis-ball coil. We conclude that it is not feasible to design a 4-mirror TLM system using tennis-ball windings.

Summary and Conclusions

The analytic theory of TLM fields in the neighbourhood of a curved, planar magnetic axis shows that the field is specified by three scalar functions a, b and g, which determine such parameters as the overall mirror ratio R, the magnetic well mirror ratio R_W and the fanning ratio F. For any field so specified, one can calculate the adiabatic invariant J defining the guiding centre drift surfaces. The J 'contours' (the curves in which the J surfaces intersect the midplane) are approximately circular and are nested about a drift axis : this drift axis is displaced radially as a result of the field bending necessary to achieve toroidal linking, and various bending strategies can be proposed to minimise this radial displacement, the most promising being to bend the field locally in R neighbourhood of the vertical fishtails of the quadrupole field.

For a given profile b(s), it is possible to specify an 'optimum' profile for the function g because this then determines R_W and F. For given midplane flux, the cost of a TLM magnet is shown to scale approximately as $(FR)^2$, and for fixed R_W this has a minimum when F lies in the range 3 - 4.

These analytic studies provide a starting point for computational studies of filamentary coil layouts which will approximately reproduce these optimum profiles in the neighbourhood of the magnetic axis. In the case of 8-mirror TLM systems, it proves possible to design configurations which approach the optimum, using 8 yin yang coils laid out along an approximately square magnetic axis, with four additional bending coils to guide the flux around the rounded corners. Approximate optimum dimensions are derived. It also proves possible to use 8 tennis-ball coils, each of which can be built up out of three flat coils. However the resulting field configuration is significantly inferior to the yin yang design. It is also possible to design a 4-mirror configuration using 4 yin yang coils plus eight bending coils : the corresponding 4-tennis-ball coil configuration proves to have unacceptable adverse toroidal effects.

Acknowledgements

The analytic part of this paper was substantially influenced by discussions with J. Votruba, who also wrote the computer programs used to prepare figs. 1 - 4. The computations described in sections 5 - 7 were made possible by the Culham magnetic field design programme MAGINT, written by T.J. Martin, and we are most grateful to him for developing it with this application in mind. We also acknowledge the help given by P. Kirby in investigating the drift orbits referred to in section 7.

References

1. J.G. Cordey, C.J.H. Watson, Toroidally Linked Mirror Reactor Design, Proc. IAEA Workshop Fusion Reactor Design Problems, Nucl. Fusion Suppt. p.199 (1974).
2. H.P. Furth, M.N. Rosenbluth, Phys. Fluids 7, 764 (1964).
3. L.S. Hall, B. McNamara, Phys. Fluids 18, 552 (1975).
4. J.G. Cordey, C.J.H. Watson, Proc. 5th. IAEA Conf. Plasma Physics, Tokyo, IAEA-CN-33/H5 - 1 (1975).
5. J.B. Taylor, Phys. Fluids 7, 767 (1964).
6. J.D. Jukes, J. Nucl. Energy Pt. C, 6, 84 (1964).
7. L.S. Solovyev, V.D. Shafranov, Problems of Plasma Physics 5, (1967).
8. A. Erdelyi et al., Higher Transcendental Functions Vol. I, p.122.
9. E.W. Hobson, Spherical and Ellipsoidal Harmonics, Chelsea 1955.
10. B. McNamara, private communication.
11. J.G. Cordey, C.J.H. Watson, Proc. BNES Conf. on Nuclear Fusion Reactors, Culham 1969, p. 122.
12. M.A. Peterson et al., UCRL 75826.
13. T.H. Batzer et al., UCRL 51617.
14. P. Kirby and C.J.H. Watson, to be published.

Table I

H = 8

L = 5.5 A = 100°			L = 5.0 A = 110°			L = 4.5 A = 120°	
CS	CT		CR	CI		CQ	CP
W = 2.7	W = 3.5		W = 2.4	W = 3.2		W = 2.15	W = 2.8
R = 2.95	R = 2.11		R = 3.01	R = 2.05		R = 3.01	R = 2.05
Δ = 0.00	Δ = 0.01	8Y3	Δ = 0.025	Δ = 0.02	8Y2	Δ = 0.02	Δ = 0.03
F = 2.4	F = 2.4		F = 3.2	F = 3.0		F = 5.4	F = 4.2
R_x = 1.9	R_x = 1.5		R_x = 2.1	R_x = 1.7		R_x = 2.35	R_x = 1.9
I = 7.6	I = 6.25		I = 7.5	I = 6.0		I = 7.25	I = 5.9

H = 6

L = 5 A = 100°			L = 4 A = 110°			L = 3.75 A = 120°	
DE	DF		DG	DH		DB	DA
W = 2.2	W = 2.8		W = 1.9	W = 2.5		W = 1.7	W = 2.2
R = 2.97	R = 2.10		R = 3.05	R = 2.0		R = 3.08	R = 2.04
Δ = 0.02	Δ = 0.05		Δ = 0.02	Δ = 0.02		Δ = 0.02	Δ = 0.02
F = 7.5	F = 5.4		F = 9	F = 6.7		F = 9.0	F = 7.8
R_x = 2	R_x = 1.7		R_x = 2.8	R_x = 1.85		R_x = 3	R_x = 2
I = 7.2	I = 6.0		I = 6.9	I = 5.55		I = 6.7	I = 5.45

8 mirror Yin yang configurations

Centre at (4, - 11): separation S = 7.5

F defined by lines starting at (4.25, - 10.25) and (4.75, - 10.75)

Table II

H =	G = 4.15	4.45	4.9
8	FM R = 3.03 Δ = 0.36 F = 6.1 R_x = 2.1 I = 18.0	FN R = 2.5 Δ = 0.25 F = 4.8 R_x = 1.75 I = 15.8	FO R = 2.03 Δ = 0.15 F = 3.9 R_x = 1.5 I = 13.5
9	FP R = 3.04 Δ = 0.24 F = 4.8 R_x = 1.8 I = 18.1	FQ R = 2.52 Δ = 0.14 F = 4.0 R_x = 1.6 I = 15.9	FR R = 2.05 [8T2] Δ = 0.08 F = 3.4 R_x = 1.45 I = 13.6
10	FJ R = 2.99 [8T3] Δ = 0.13 F = 4.1 R_x = 1.7 I = 18.0	FK R = 2.53 Δ = 0.08 F = 3.6 R_x = 1.45 I = 15.8	FL R = 2.03 Δ = 0.02 F = 3.15 R_x = 1.35 I = 13.6
11	FS R = 2.95 Δ = 0.045 F = 3.8 R_x = 1.5 I = 17.8	FT R = 2.49 Δ = 0.01 F = 3.35 R_x = 1.4 I = 15.7	FU R = 2.02 Δ = -0.01 R_x = 1 I = 13.6

8-mirror Tennis-ball seam configurations

Centre at (4, - 11): length L = 6

F defined by lines starting at (3.95, - 10.95) and (4.45, - 11.45)

Captions

Figs. 1 and 2

The correspondence between the parameters C_1 and C_3 in the expression for g and the fanning parameter F and the critical mirror ratios R_W and R_J

----- R_W and F for fixed C_1 and C_3, as labelled

—·—·— R_J for peaked g profile (with C_3 chosen so that (6.3) is just satisfied at midplane) and flat g profile (with C_3 chosen so that $\frac{\partial^2}{\partial z^2}\frac{\partial B}{\partial \psi} = 0$ at midplane)

——— R_W for peaked and flat g profiles.

Fig. 3 $\frac{\partial B}{\partial \psi}$ profiles for various choices of g profile.

Fig. 4 Magnet cost optimisation function FR for fixed R_W, showing optimum R value.

Fig. 5 Rectangular yin yang winding
(a) plane protection
(b) conical projection

Fig. 6 An 8-yin yang coil layout TLM 8Y2 in plane projection.

Fig. 7(a) |B| contour and field line plots for 8-yin yang configuration TLM 8Y2.

Fig. 7(b) |B| contour and field line plots for 8-yin yang configuration TLM 8Y3.

Fig. 8 Rectangular tennis-ball seam winding constructed out of three flat coils
(a) plan view of the three coils
(b) projection onto horizontal plane
(c) conical projection showing direction of current flow.

Fig. 9(a) |B| contour and field line plots for 8-tennis-ball configuration TLM 8T2.

Fig. 9(b) |B| contour and field line plots for 8-tennis-ball configuration TLM 8T3.

Fig. 10 A 4-yin yang coil layout with 45° tilting of the coil axes.

Fig. 11 |B| contour and field line plots for 45° tilted 4-yin yang configuration.

Fig. 12 A 4-yin yang coil layout with no tilting of the coil axes plane projection: separation of axes = 8 m, two bending coils.

Fig. 13 |B| contour and field line plots for 4-yin yang configurations: separation of axes = 8 m.

Fig. 14 A 4-yin yang coil layout TLM 4Y3 with separation of axes = 14 m and eight bending coils.

Fig. 15 |B| contour and field line plots for configuration TLM 4Y3.

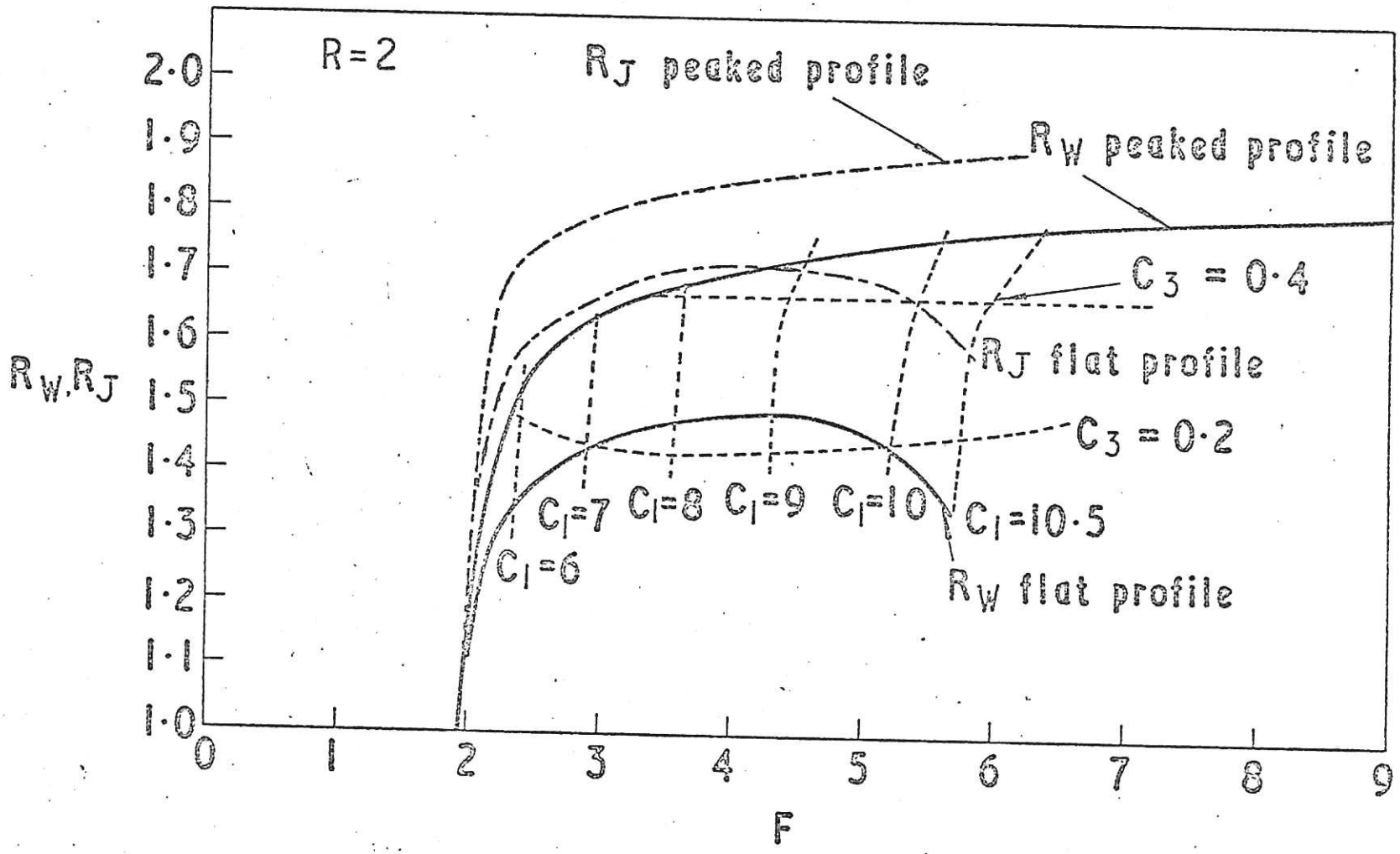
R=2
R_J peaked profile
R_W peaked profile
$C_3 = 0.4$
R_J flat profile
$C_3 = 0.2$
$C_1=7$ $C_1=8$ $C_1=9$ $C_1=10$ $C_1=10.5$
$C_1=6$
R_W flat profile
R_W, R_J
2·0
1·9
1·8
1·7
1·6
1·5
1·4
1·3
1·2
1·1
1·0
0 1 2 3 4 5 6 7 8 9
F

Fig. 1

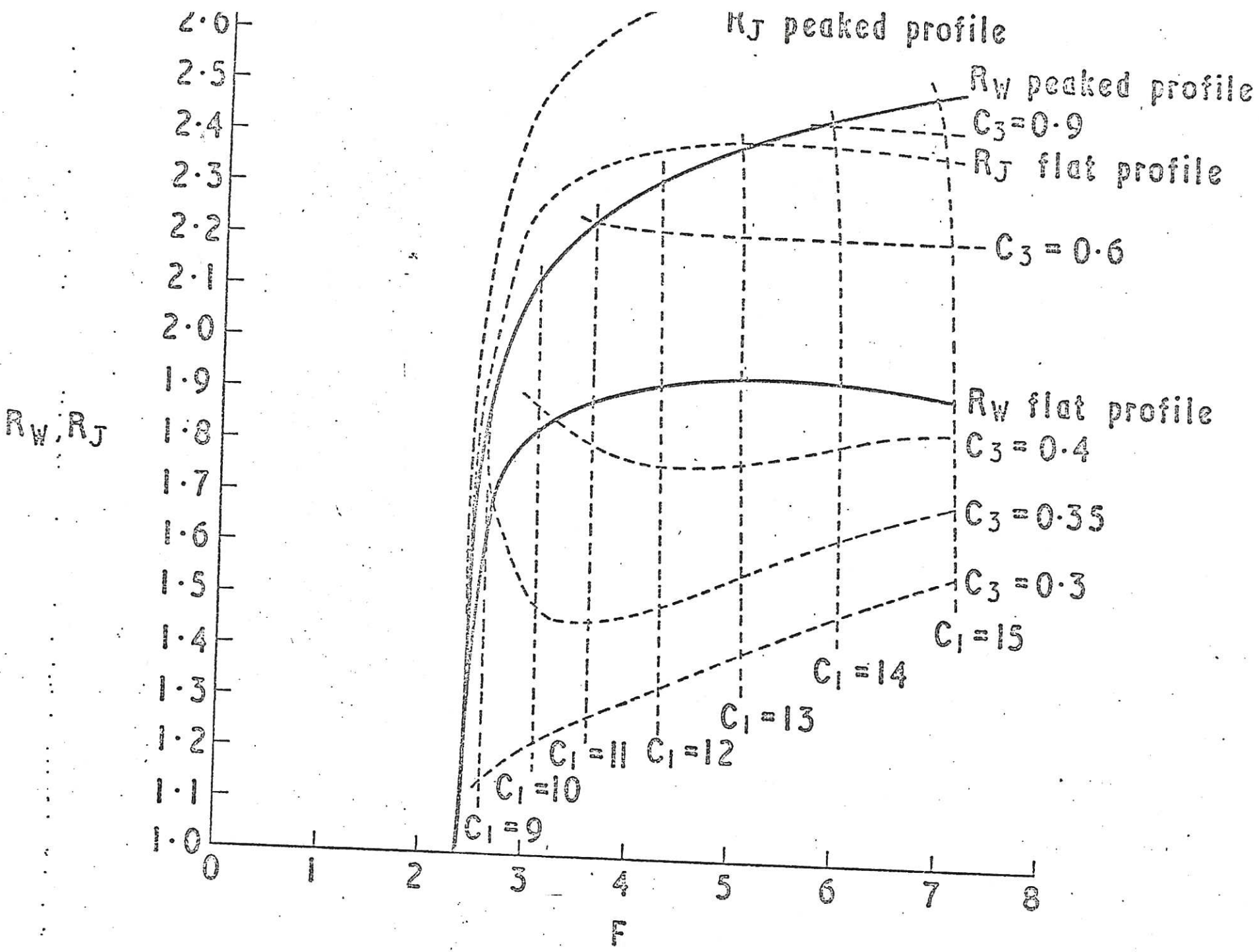
R_J peaked profile
R_W peaked profile
$C_3 = 0.9$
R_J flat profile
$C_3 = 0.6$
R_W flat profile
$C_3 = 0.4$
$C_3 = 0.35$
$C_3 = 0.3$
$C_1 = 15$
$C_1 = 14$
$C_1 = 13$
$C_1 = 12$
$C_1 = 11$
$C_1 = 10$
$C_1 = 9$
R_W, R_J
F
2·6
2·5
2·4
2·3
2·2
2·1
2·0
1·9
1·8
1·7
1·6
1·5
1·4
1·3
1·2
1·1
1·0
0
1
2
3
4
5
6
7
8

Fig. 2

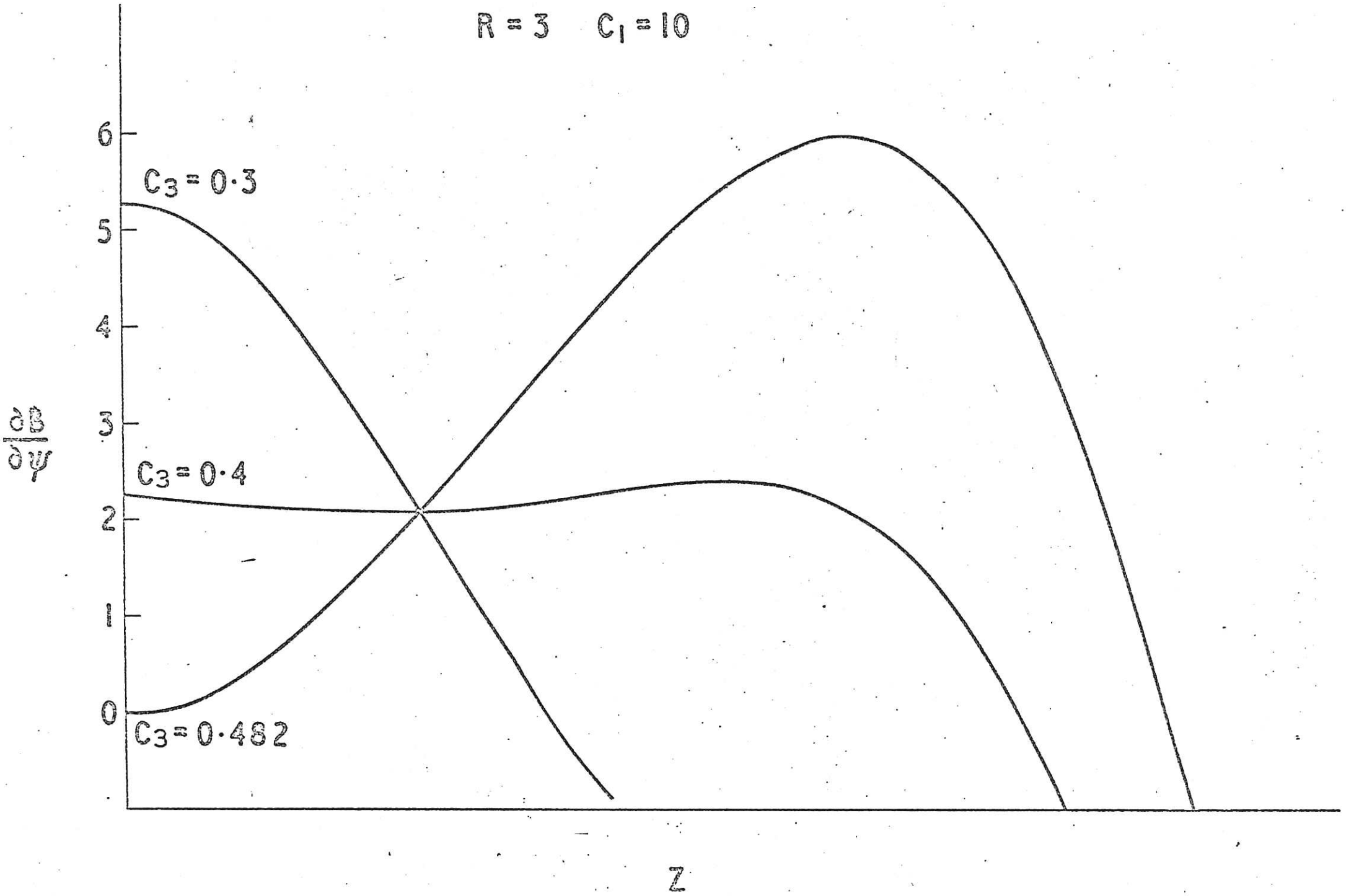

Fig. 3

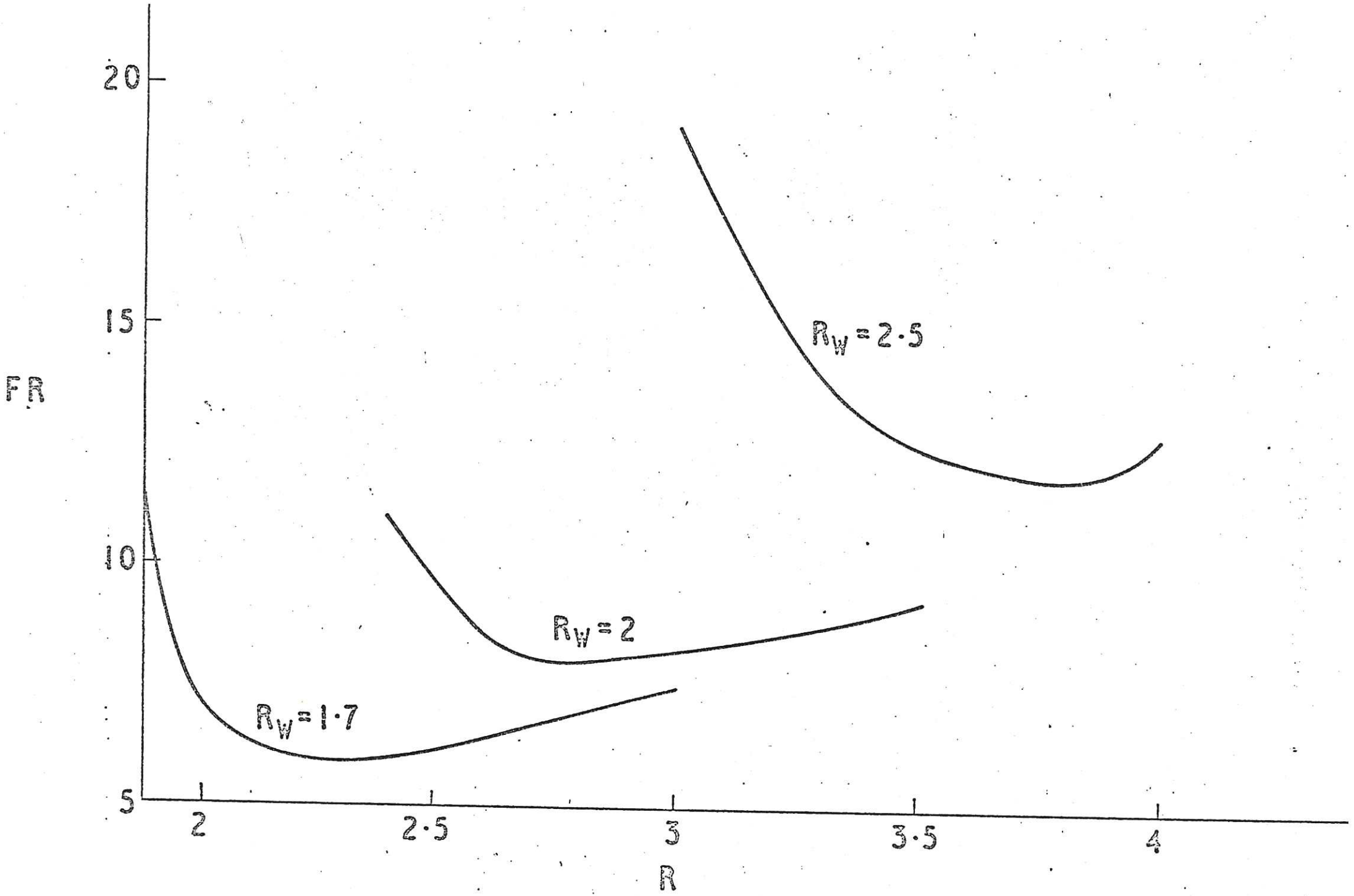

Fig. 4

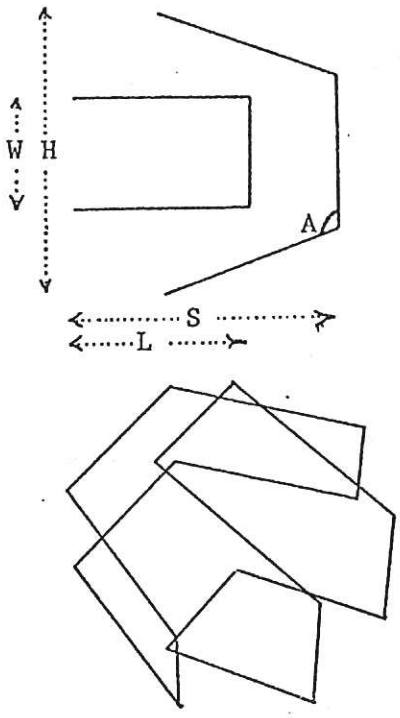

(a)

(b)

Fig. 5 : Rectangular yin yang winding

(a) plane projection

(b) conical projection

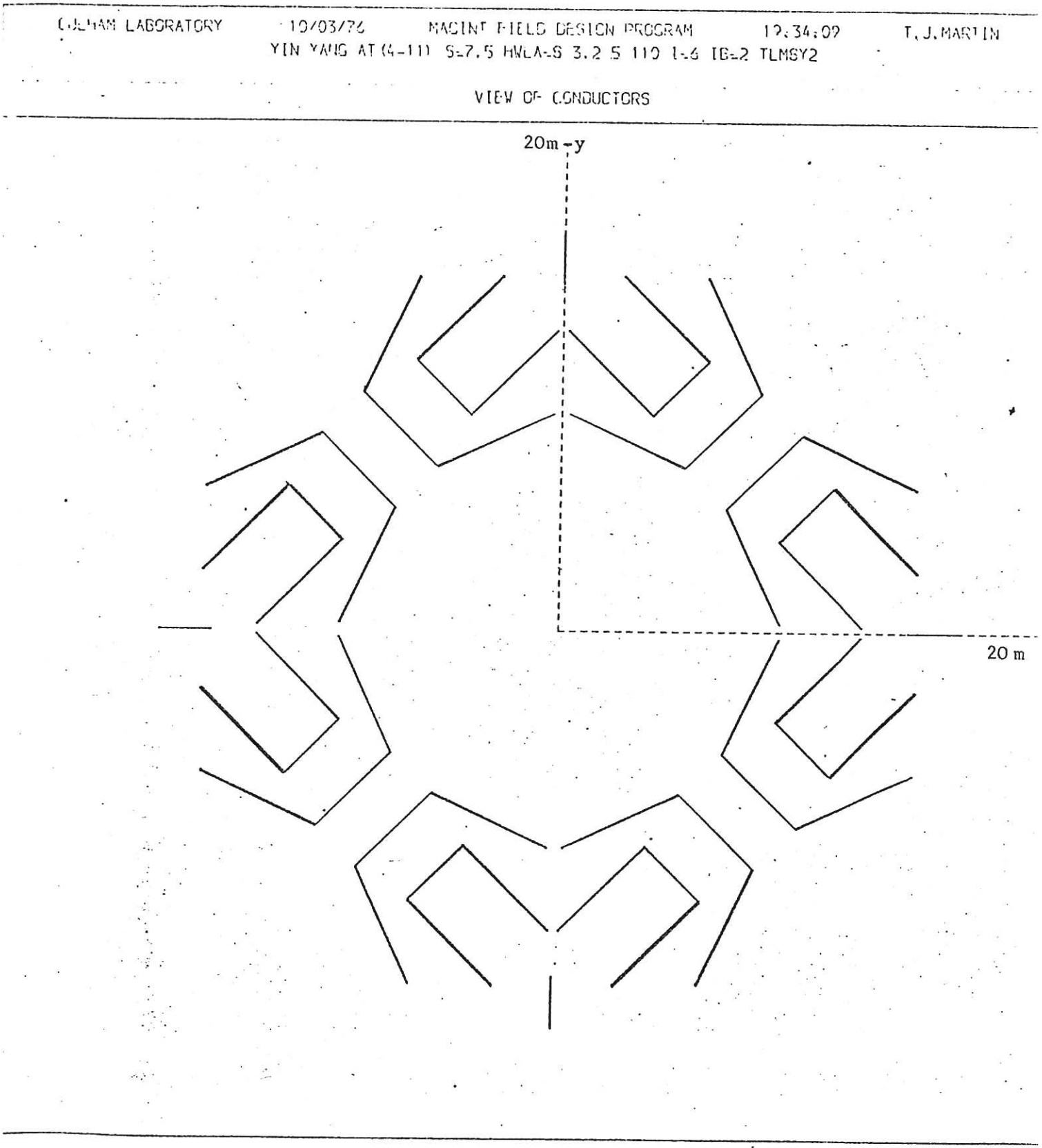

Fig. 6: An 8-yin yang coil layout in plane projection.

LHAM LABORATORY 16/09/76 MAGINT FIELD DESIGN PROGRAM 19.18.05 T.J.MARTIN EXT.341

YIN YANG AT(4-11) S=7.5 HWLA=8 3.2 5 110 I=6 IB=2 TLM8Y2

MOD(B) CONTOURS ON PLANE

(0.000-18.000 0.000), (18.000-18.000 0.000), (0.000 0.000 0.000)

MIN= 0.1447E-06 MAX= 0.1472E02

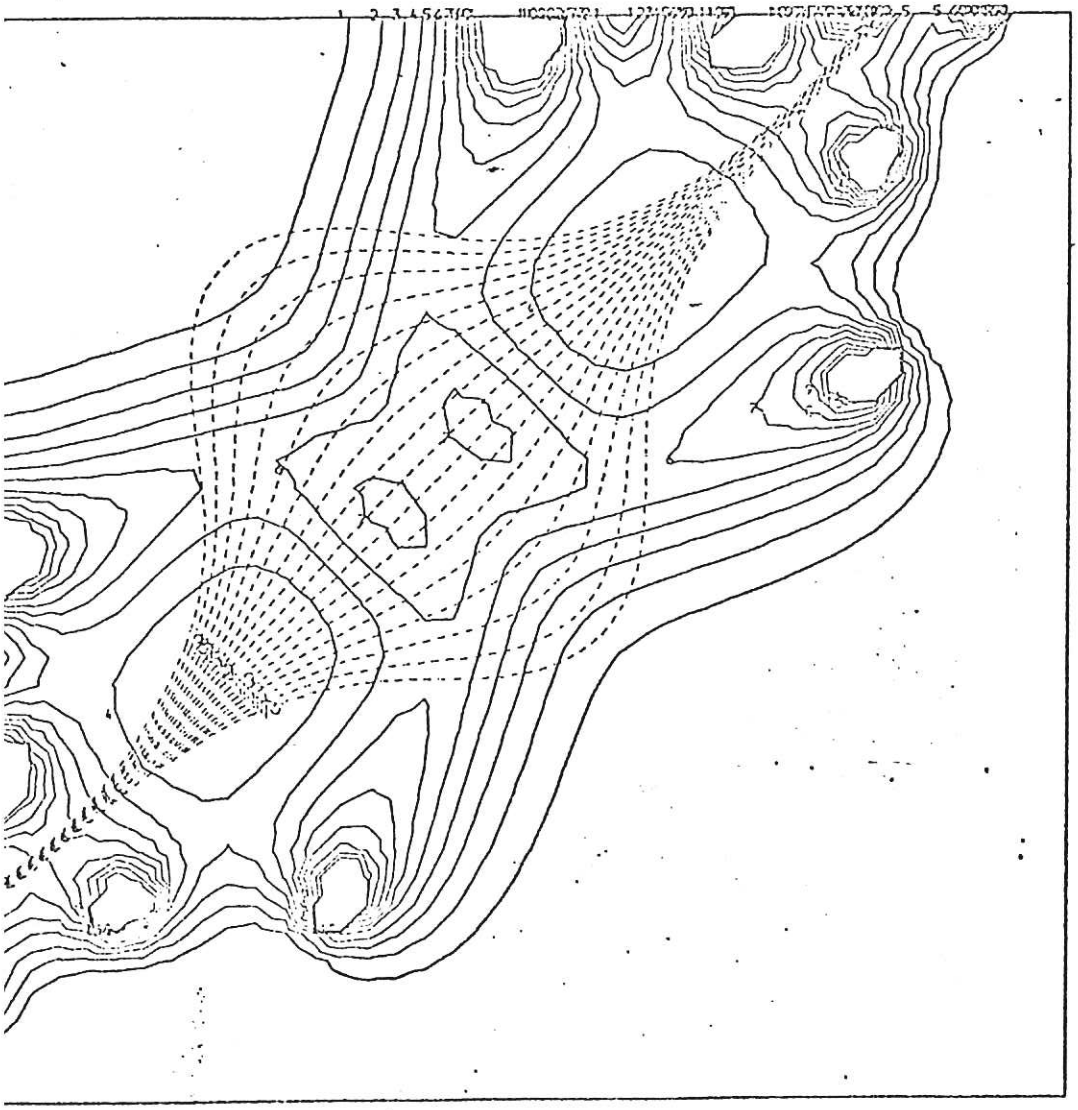

1	0.5000E00
2	0.7500E00
3	0.1000E01
4	0.1250E01
5	0.1500E01
6	0.1750E01
7	0.2000E01
8	0.2250E01
9	0.2500E01
10	0.2750E01
11	0.3000E01

Fig. 7(a)

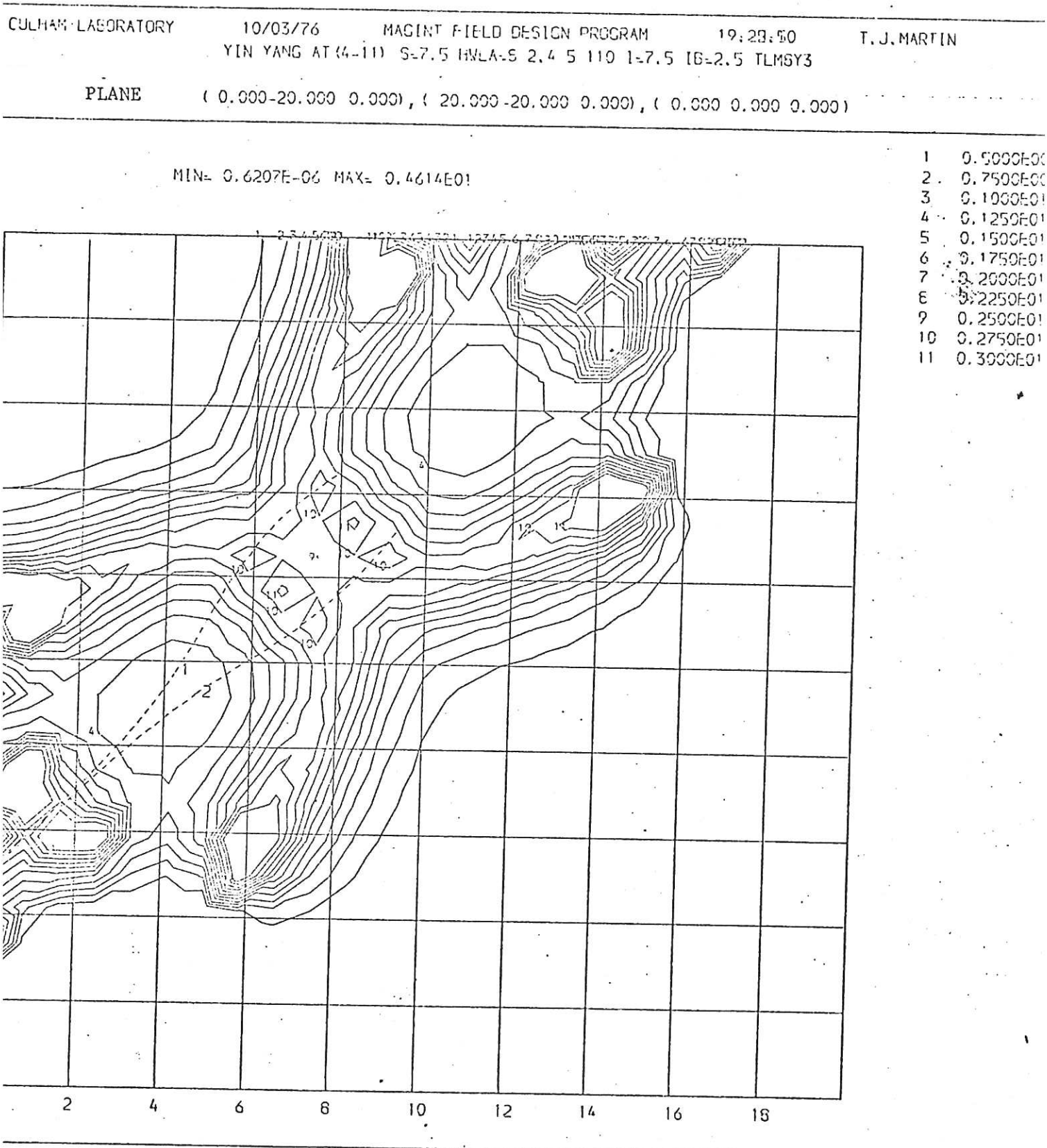

Fig. 7(b): $|B|$ contour and field line plots for 8-yin yang configuration 8Y3.

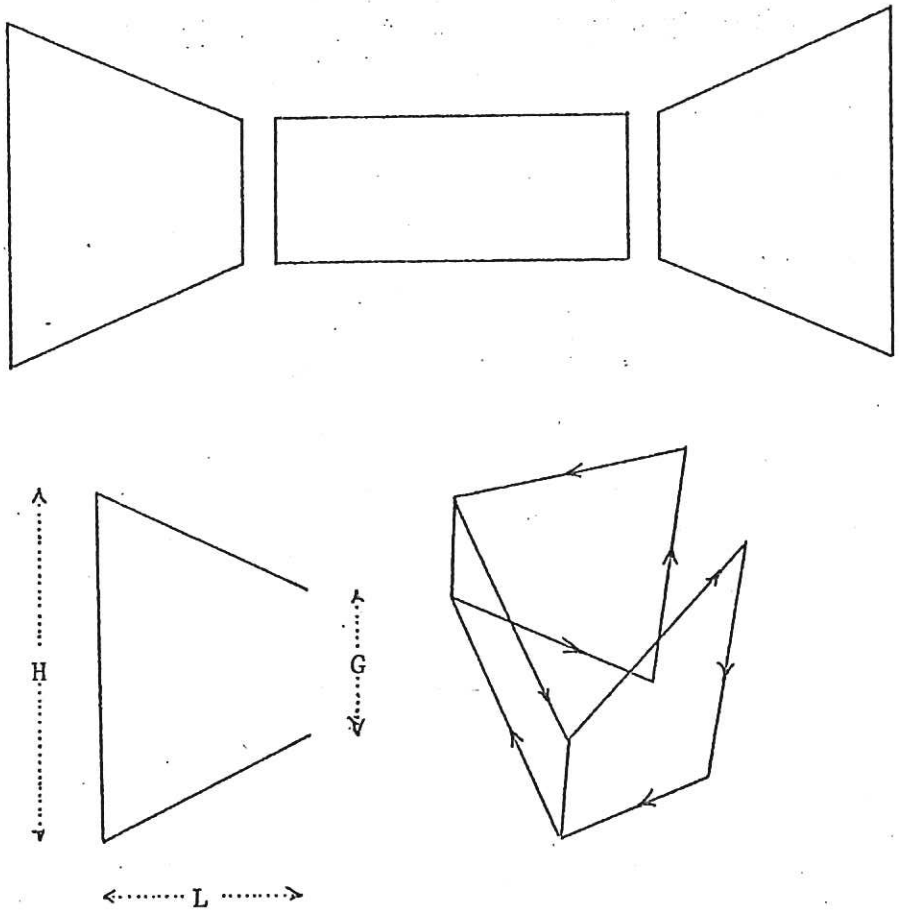

Fig. 8: Rectangular tennis-ball seam winding constructed out of three flat coils

(a) plan view of the three coils

(b) projection onto horizontal plane

(c) conical projection showing direction of current flow

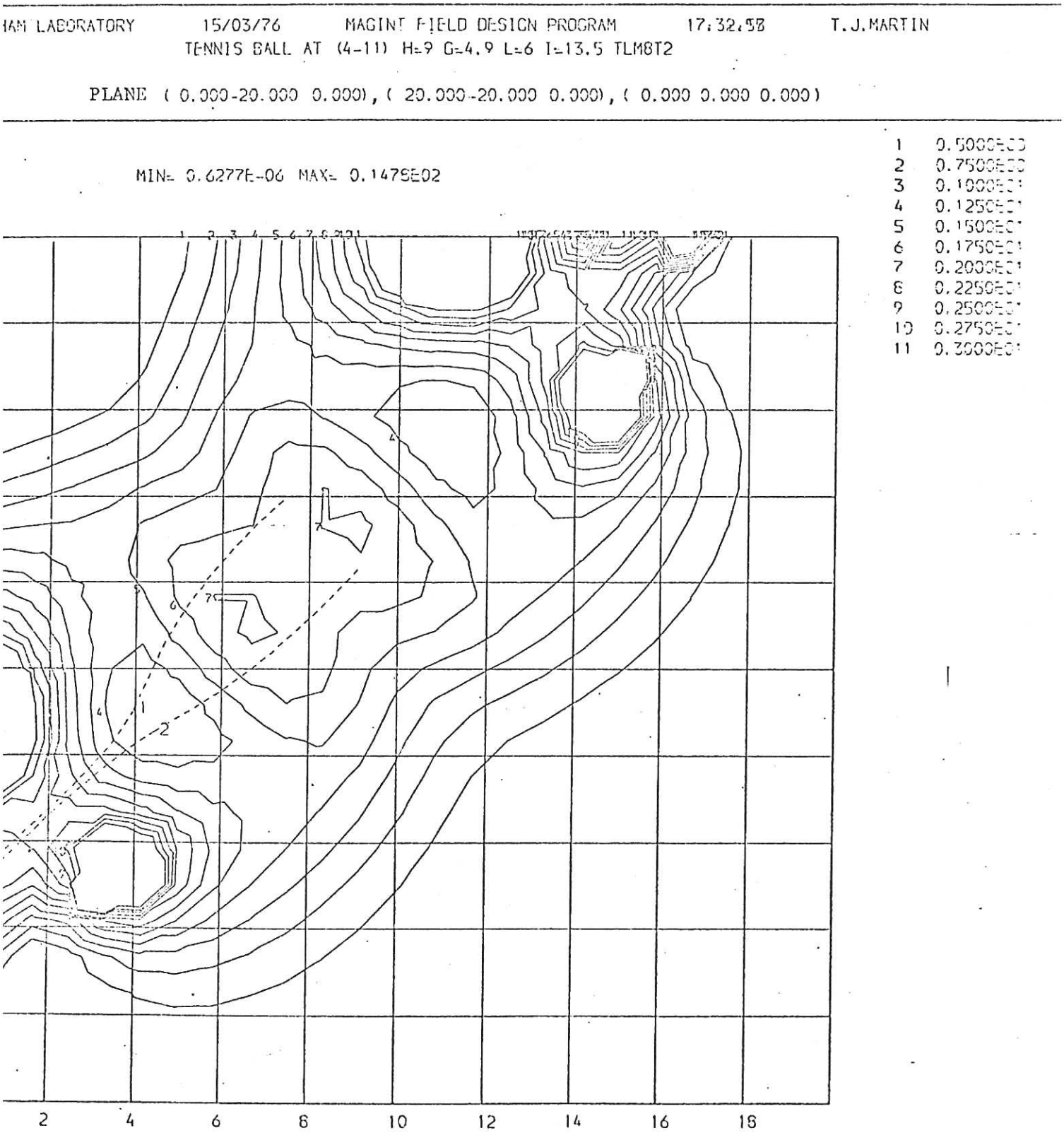

Fig. 9(a): |B| contour and field line plots for 8-tennis-ball configuration 8T2.

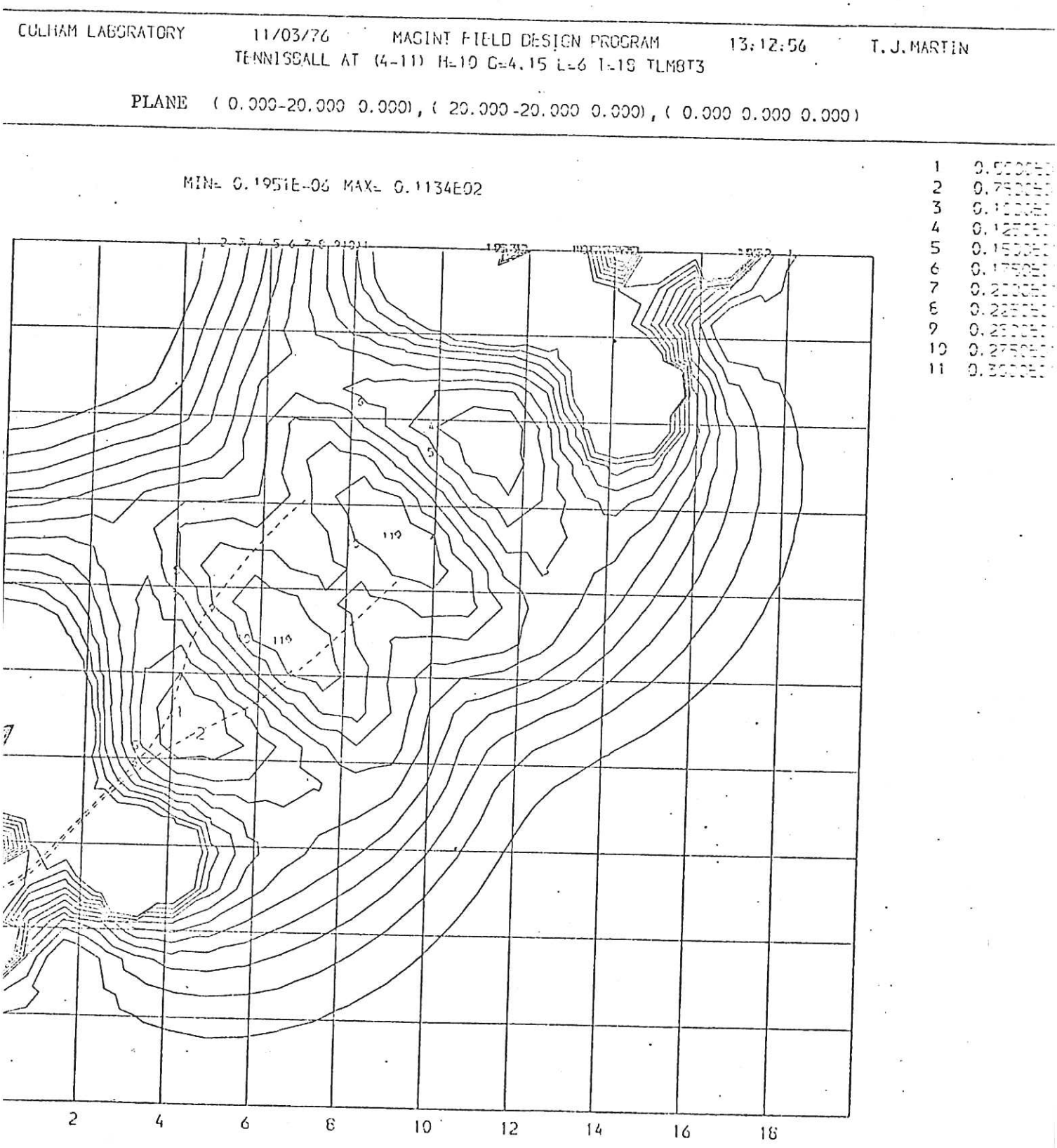

Fig. 9(b): |B| contour and field line plots for 8-tennis-ball configuration 8T3.

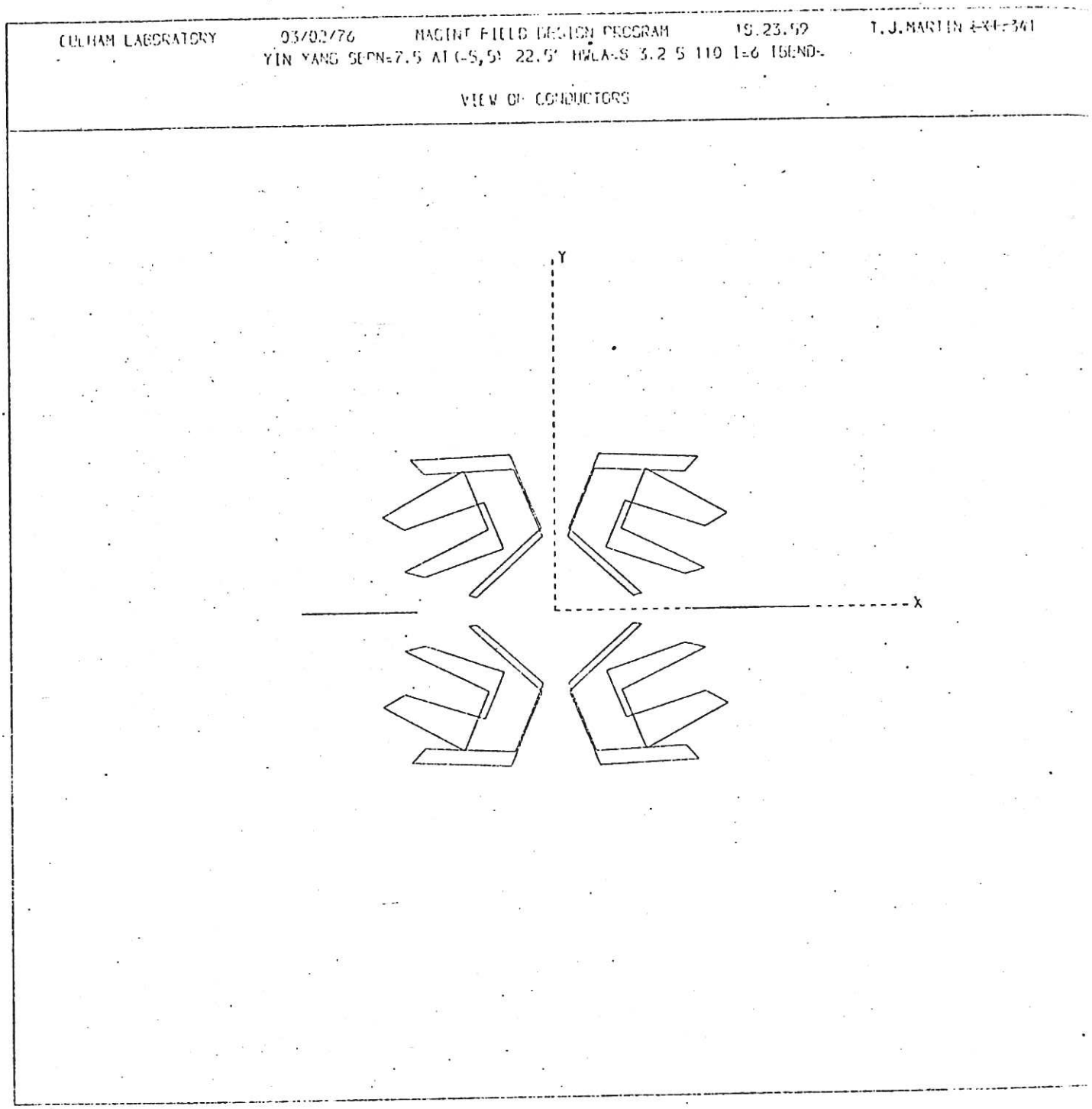

Fig.10: A 4-yin yang coil layout with 45° tilting of the coil axes.

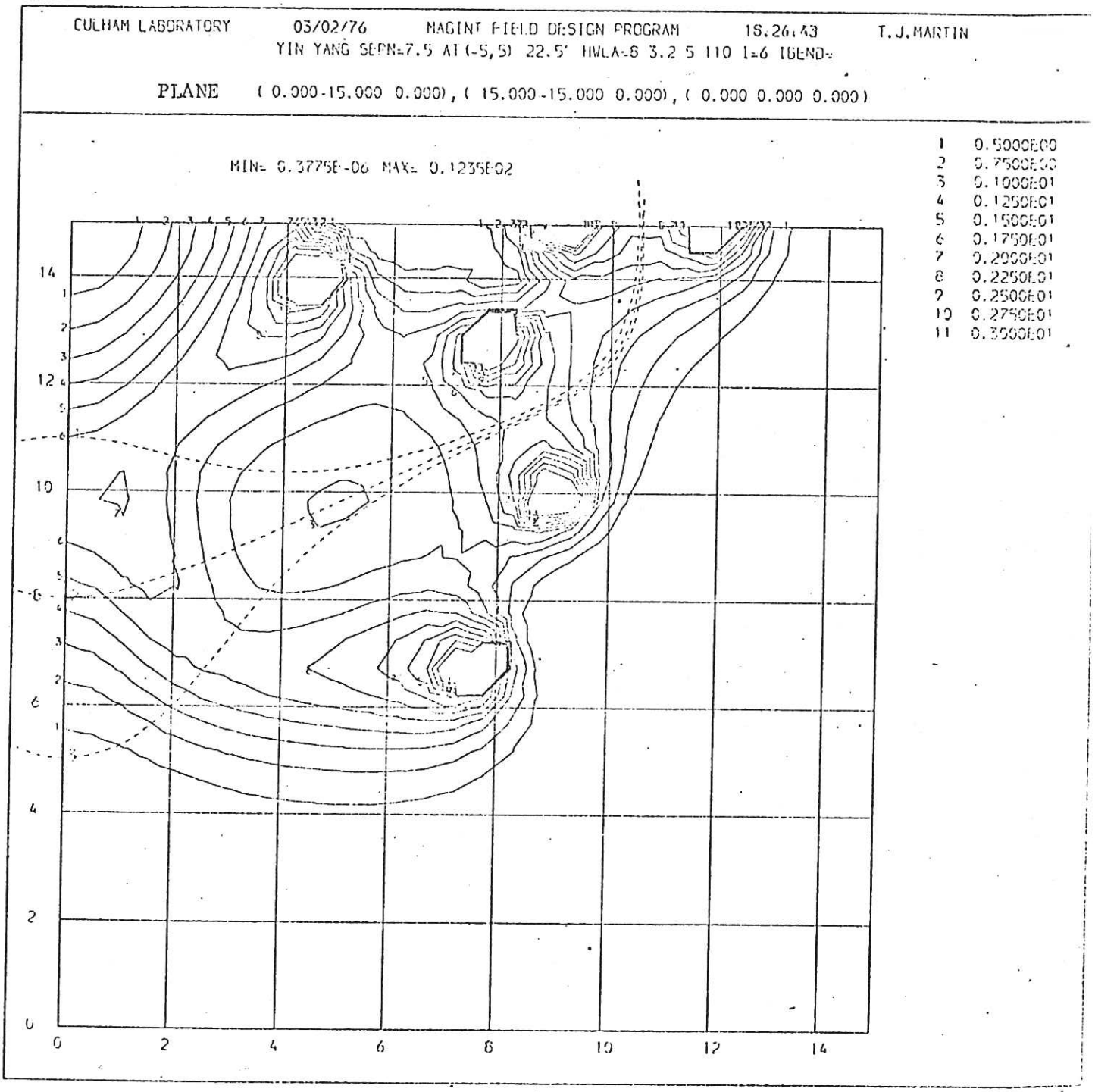

Fig. 11: |B| contour and field line plots for 45° tilted 4-yin yang configurations.

YIN YANG S=7.5 AT(-4.75,4) HWLA=S 2.2 5 110 I=7 IBEND=15 4Y3

VIEW OF CONDUCTORS

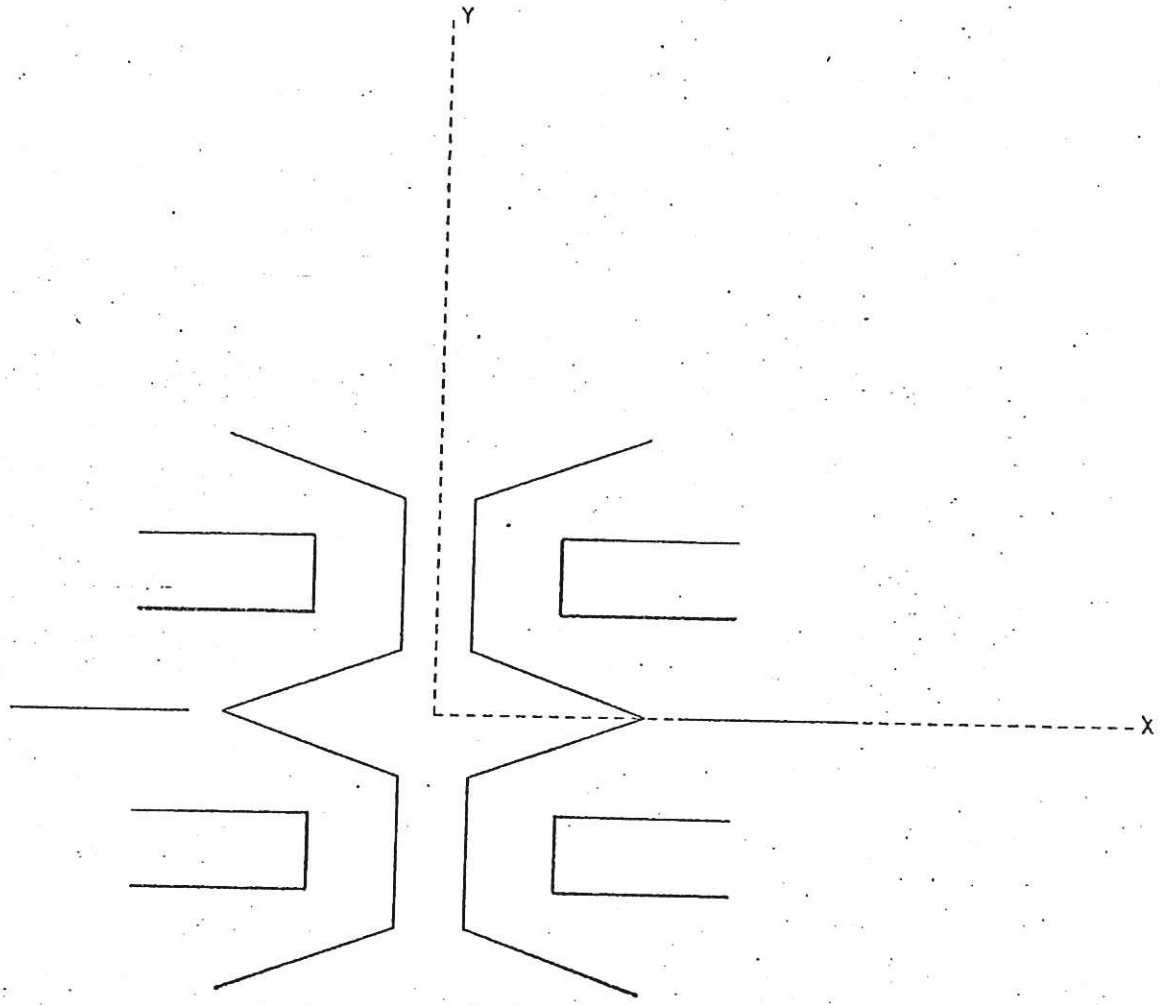

Fig.12 A 4-yin yang coil layout with no tilting of the coil axes plane projection.

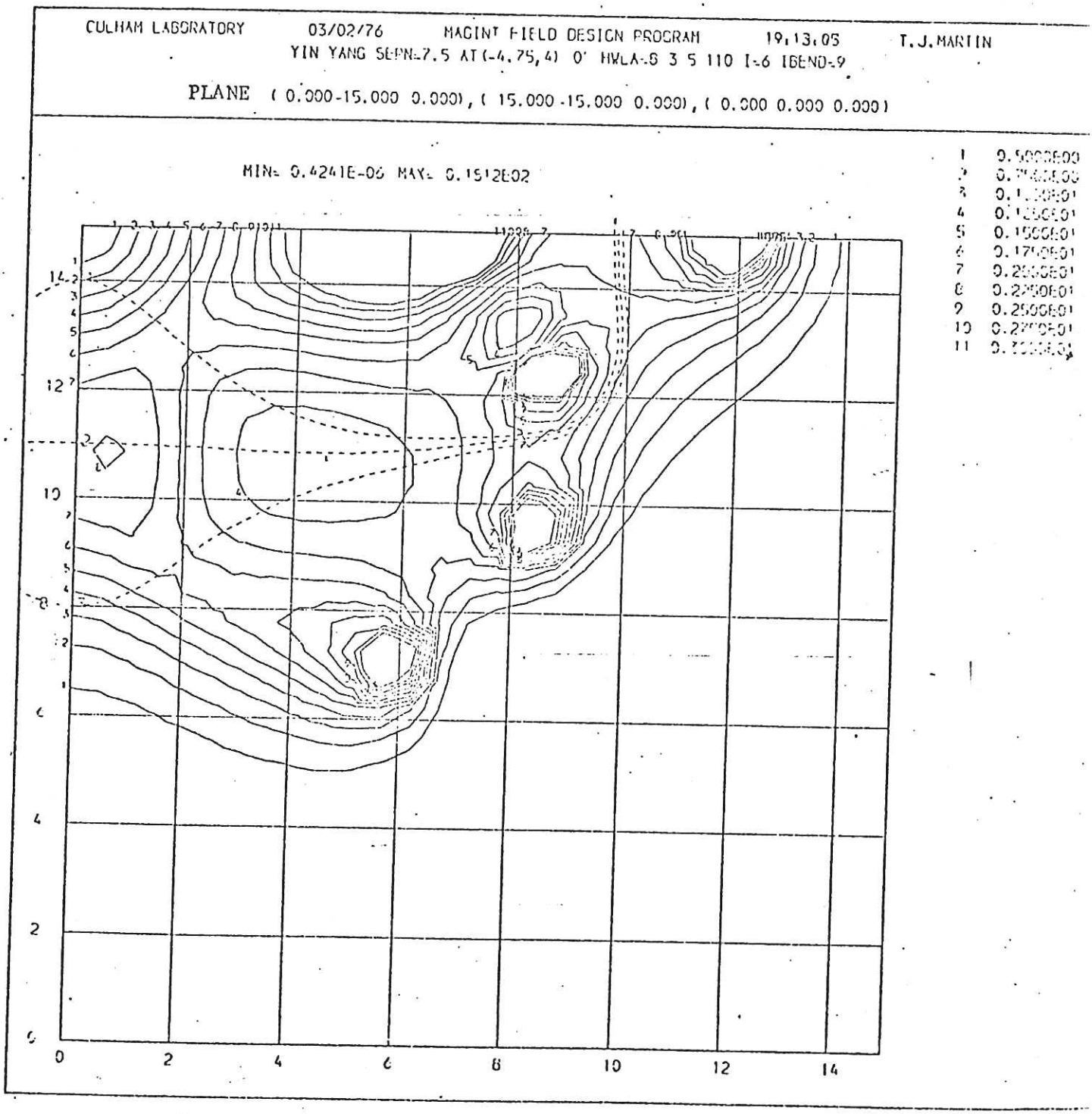

Fig.13 : $|B|$ contour and field line plots for 4-yin yang configurations

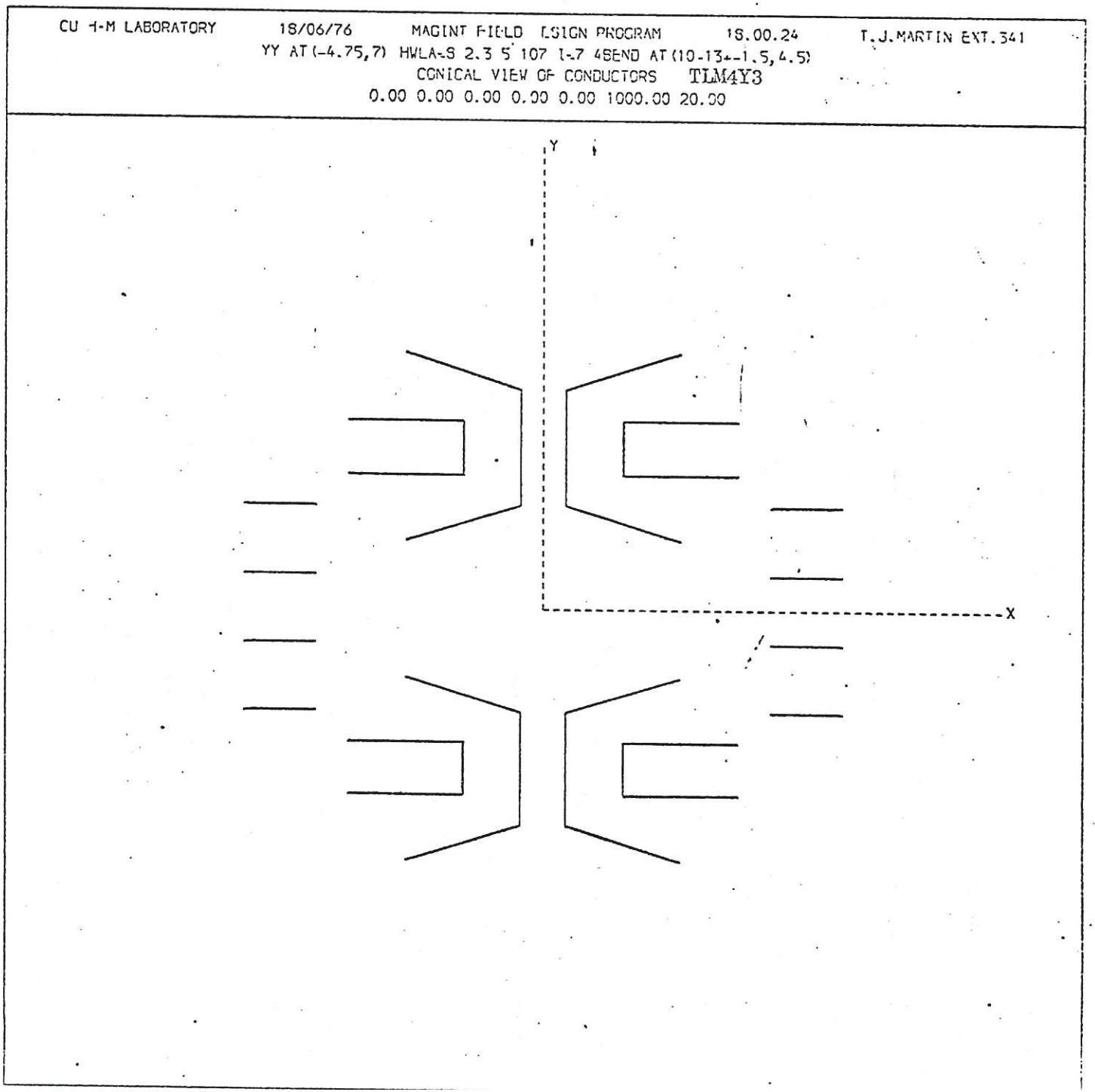
CU H-M LABORATORY 18/06/76 MAGINT FIELD DSIGN PROGRAM 18.00.24 T.J.MARTIN EXT.341
YY AT(-4.75,7) HWLA-S 2.3 5 107 1-7 4BEND AT(10-134-1.5,4.5)
CONICAL VIEW OF CONDUCTORS TLM4Y3
0.00 0.00 0.00 0.00 0.00 1000.00 20.00
Y
X

Fig. 14

CULHAM LABORATORY 16/09/76 MAGINT FIELD DESIGN PROGRAM 18.25.17 T.J.MARTIN EXT.341
YY AT(-4.75,7) HVLA-8 2.3 5 107 1-7 4SEND AT(10-13+-1.5,4.5) TLM4Y3
MOD(B) CONTOURS ON PLANE
(0.000-13.000 0.000), (15.000-13.000 0.000), (0.000 0.000 0.000)

MIN= 0.4806E-06 MAX= 0.1041E02

1	0.5000E00
2	0.7500E00
3	0.1000E01
4	0.1250E01
5	0.1500E01
6	0.1750E01
7	0.2000E01
8	0.2250E01
9	0.2500E01
10	0.2750E01
11	0.3000E01

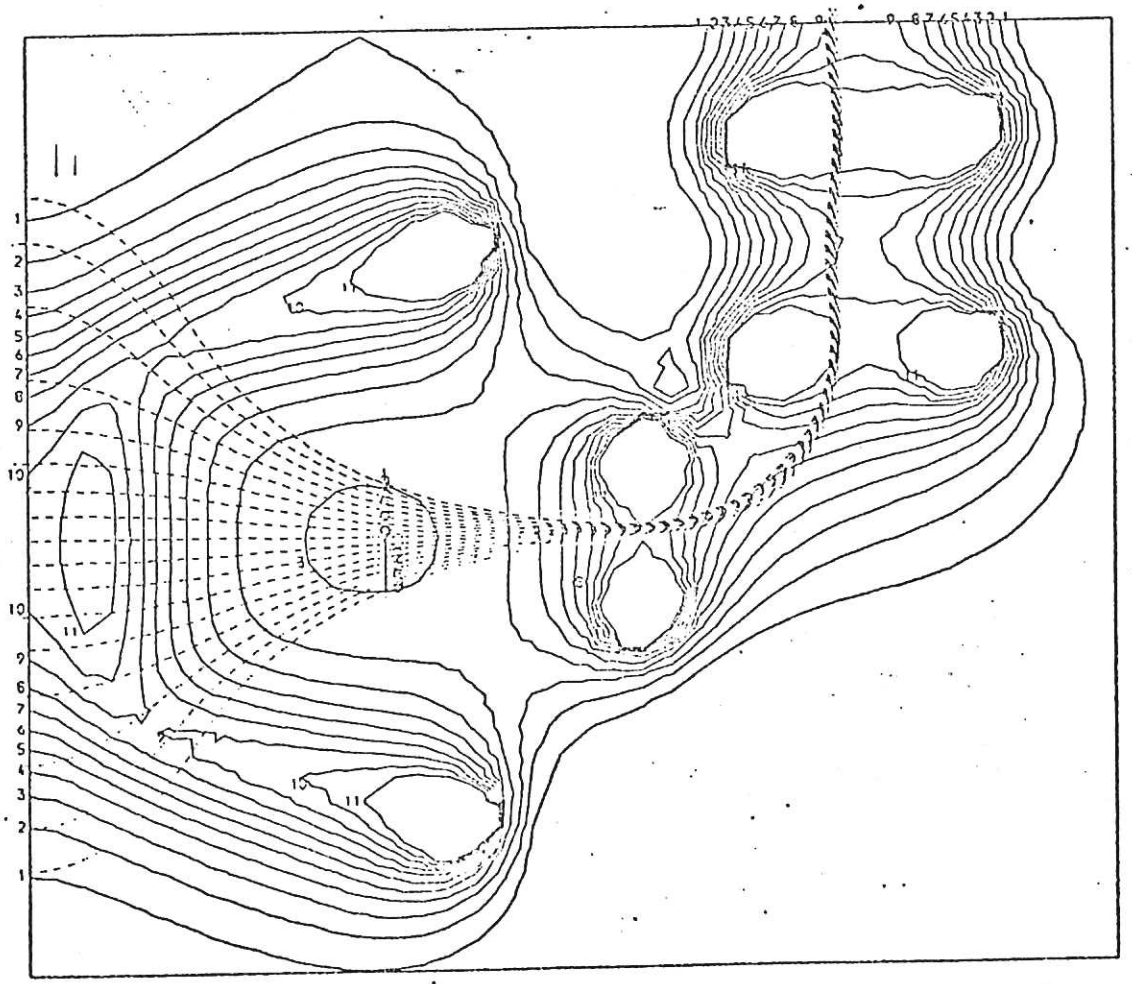

Fig. 15